TETRACARBONYL[N,N'-BIS(FERROCENYLMETHYLENE) ETHYLENEDIAMINE]CHROMIUM(0), $Cr(CO)_4$(BFEDA): SYNTHESIS AND CHARACTERIZATION

A THESIS SUBMITTED TO
THE GRADUATE SCHOOL OF NATURAL AND APPLIED SCIENCES
OF
MIDDLE EAST TECHNICAL UNIVERSITY

BY

CEYHUN AKYOL

IN PARTIAL FULFILLMENT OF THE REQUIREMENTS
FOR
THE DEGREE OF MASTER OF SCIENCE
IN
CHEMISTRY

MARCH 2005

Approval of the Graduate School of Natural and Applied Sciences

_____

Prof.Dr. Canan Özgen

Director

I certify that this thesis satisfies all the requirements as a thesis for the degree of Master of Science.

_____

Prof. Dr. Hüseyin İşçi

Head of the department

This is to certify that we have read this thesis and that in our opinion it is fully adequate, in scope and quality, as a thesis for the degree of Master of Science.

_____

Prof. Dr. Saim Özkâr

Supervisor

Examining Committee Members

Prof. Dr. Hüseyin İşçi	(METU,CHEM)	_____
Prof. Dr. Saim Özkâr	(METU,CHEM)	_____
Prof. Dr. H. Ceyhan Kayran	(METU,CHEM)	_____
Prof. Dr. Birgül Karan	(Hacettepe Unv.,CHEM)	_____
Prof. Dr. Ahmet M. Önal	(METU,CHEM)	_____

I hereby declare that all information in this document has been obtained and presented in accordance with academic rules and ethical conduct. I also declare that, as required by these rules and conduct, I have fully cited and referenced all material and results that are not original to this work.

Name, Last name :

Signature :

ABSTRACT

TETRACARBONYL[N,N'-BIS(FERROCENYLMETHYLENE)
ETHYLENEDIAMINE]CHROMIUM(0), $Cr(CO)_4$(BFEDA):
SYNTHESIS AND CHARACTERIZATION

Akyol, Ceyhun
M.S., Department of Chemistry
Supervisor: Prof. Dr. Saim Özkâr

March 2005, 63 pages

N,N'-bis(ferrocenylmethylene)ethylenediamine was prepared from the reaction of ferrocenecarboxaldehyde and ethylenediamine and characterized by IR, Raman, ^{1}H and ^{13}C-NMR spectroscopy. The electrochemical behaviour of this ligand was also studied for the first time by cyclic voltammetry. Diferrocenyl diimine ligand was used in the thermal substitution of 1,5-cyclooctadiene in $Cr(CO)_4(\eta^{2:2}$-1,5-cyclooctadiene) at 38°C in toluene for two hours to form the tetracarbonyl[N,N'-bis(ferrocenylmethylene)ethylenediamine]chromium(0), [$Cr(CO)_4$(BFEDA)]. This complex was succesfully isolated and crystallized from its 1:1 toluene/dichloromethane solution and characterized by elemental analysis, MS, IR,

^{1}H, ^{13}C-NMR spectroscopy. Electrochemical behaviour of the complex was also studied by cyclic voltammetry and the mechanism of electrode reaction was investigated by in-situ UV-VIS and IR spectroscopy measurements.

This new complex has the iron atom of ferrocene unit in conjugation with the chromium metal center and, therefore, shows an electronic communication between two metal atoms.

Keywords: Ferrocenyl ligands; Diimine ligands; Carbonyl; Chromium; Ligand substitution; Electrochemistry.

ÖZ

TETRAKARBONİL[N,N'-
BİS(FERROSENİLMETİLİN)ETİLENDİAMİN]KROM(0)
KOMPLEKSİNİN SENTEZİ VE KARAKTERİZASYONU

Akyol, Ceyhun
Yüksek Lisans, Kimya Bölümü
Tez Yöneticisi: Prof. Dr. Saim Özkâr

Mart 2005, 63 sayfa

N,N'-bis(ferrosenilmetilin)etilendiamin, ferrosenkarboksaldehit ile etilendiaminin tepkimesinden hazırlandı ve IR, Raman, ^{1}H and ^{13}C-NMR spektroskopi metotları ile karakterizasyonu yapıldı. Bu ligandın elektrokimyasal davranışları ilk kez dönüşümlü voltametri ile incelendi. Elde edilen diferrosenildiimin ligandı daha sonra $Cr(CO)_4(\eta^{2,2}$-1,5-siklooktadien) kompleksi ile 38°C'de iki saat tepkimeye sokularak tetrakarbonil[N,N'-bis(ferrosenilmetilin)etilendiamin]krom(0) kompleksi elde edildi. Oluşan kompleks başarılı bir şekilde izole edildi ve 1:1 toluen/diklorometan çözeltisinde kristallendirildi ve elemental analiz, MS, IR, ^{1}H, ^{13}C-NMR spektroskopi metotlarıyla

karakterize edildi. Kompleksin elektrokimyasal davranışları da ayrıca dönüşümlü voltametri ile çalışıldı ve elektrot tepkimesinin mekanizması UV-VIS ve IR spektroskopi teknikleri kullanılarak incelendi.

Elde edilen bu yeni komplekste ferrosen birimindeki demir atomu krom metal merkezi ile konjüge haldedir ve, bundan dolayı, iki metal atomu arasında elektronik bir iletişim bulunmaktadır.

Anahtar kelimeler: Ferrosenil ligantlar; diimin ligantlar; karbonil; krom; ligant yerdeğiştirme; elektrokimya.

ACKNOWLEDGEMENTS

I would like to express my sincere gratitude to Prof. Dr. Saim Özkâr for his great support, supervision and understanding throughout in this study.

I would like to express my gratitude to Prof. Dr. Ahmet M. Önal for his helps and suggestions and valuable criticism in the progress of this work especially during the electrochemical studies.

I would like to thank Fatma Alper, Ercan Bayram, Pelin Edinç, Sanem Koçak, Cüneyt Kavaklı, Mehmet Zahmakıran, Murat Rakap, Dilek Ayşe Boğa, and Ezgi Keçeli for their caring, never ending helps and their encouragement during my study.

I also give my thanks to the members of the Chemistry Department of Middle East Technical University for providing facilities used in this study.

The last but not least, I would like to extend my gratitude to my father, İsmail, my mother, Ayşe, and my sister, Ceren, for helping me with every problem I encountered during the whole study.

TABLE OF CONTENTS

LIST OF TABLES

LIST OF FIGURES

LIST OF SCHEMES

SCHEME

CHAPTER 1

INTRODUCTION

Organometallic compounds are defined as substances containing direct metal – carbon bonds. The variety of organic moiety in such compounds is practically infinite, ranging from alkyl substituents to alkenes, alkynes, carbonyls, and aromatic and heterocyclic compounds.

Probably the first organometallic compound was prepared over 200 years ago, in 1760, when the French chemist L. C. Cadet attempted to make invisible ink from arsenate salt, he ended up with a repulsively smelling liquid, which was later identified as dicacodyl (=stink), As_2Me_4[1]. In 1827, the first olefin complex, $K[PtCl_3(C_2H_4)]$, known as the Zeise's salt,[2] was synthesized. More recently, the synthesis of ferrocene $(\pi\text{-}C_5H_5)_2Fe$ in 1951[3,4] and the determination of its structure in the following year (Figure 1.1),[5] opened up a field of research of hitherto unforeseen property.[6] This structural determination of ferrocene revealed an iron metal sandwiched by two parallel cyclopentadienyl (Cp) rings. Cp ligands were bonded covalently to the iron center; however, they rotated freely with respect to each other, and this 'new type of organo-iron compound' was found to be aromatic, highly stable and soluble in most common organic solvents.[7] This compound also has allowed theoreticians to gain a more profound understanding of the role of d-orbitals in determining molecular structure and properties.[8]

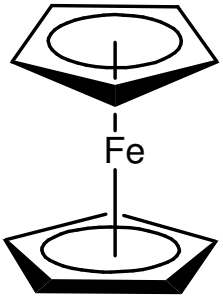

Figure 1.1. The structural formula of ferrocene

The study of ferrocene derivatives has increased exponentially during the last decade for they have been used as homogeneous catalysts,[9] molecular sensors,[10] molecular magnets,[11] non-linear optic materials[12] and liquid crystals.[13,14] Ferrocene derivatives containing atoms with good donor abilities have attracted additional interest, since the coordination of a metal to these molecules produces multicenter molecules.[15] In compounds of this kind, the presence of proximal metals may affect the properties of iron(II). For instance, it has been proven that the proclivity of the iron(II) to oxidize depends on several factors including the nature of the transition metal and the mode of coordination of the ferrocenyl unit to it.[16] Besides that, ferrocene and some of its derivatives are highly selective molecular carriers with antineoplastic properties[17] and some examples of antitumour materials containing ferrocenyl groups have also been reported.[18]

In general, three properties distinguish ferrocenyl substituents from other, purely organic moieties: (i) unique steric bulk with special steric requirements due to the cylindrical shape, (ii) electronic stabilization of adjacent electron-deficient centers due to participation of the iron atom in the dispersal of the positive charge, and (iii) chemical stability and reversibility of the ferrocene/ferricenium redox couple, which has made ferrocene one of the most classical redox agents of the organometallic chemistry.[19]

Another important class of the organometallic chemistry is the transition-metal carbonyls. The metal carbonyls are the compounds of various transition metals with carbon monoxide. These are not usually considered as organometallic compounds, although their structures do involve covalent bonds between the metal atoms and carbon atoms. The metal carbonyls are, however, similar to covalent organometallic compounds in their properties, generally either liquids or low melting solids, and even the heavier molecules have appreciable volatility at room temperature. They are generally soluble in organic solvents, but insoluble in water. The metal carbonyls are not very stable toward thermal decomposition, and most of the known carbonyls will decompose at or below 200°C, generally yielding carbon monoxide and free metal.[20]

Infrared spectra of metal carbonyls constitute a valuable source of information concerning both structure and bonding. The stretching frequency ν(CO) in carbonyls is lower than the stretching frequency of the free CO molecules due to back-bonding. The range in which the ν(CO) bands are found depends on the nature of the carbonyl groups present in the complex. For terminal CO groups ν(CO) has a higher value than it does for bridging groups. From positions of ν(CO) bands in the spectrum, the electronic structure of the M – CO fragment may be inferred, and the structure of the complex may be determined from the number of bands and their intensities. ν(CO) vibrations for M – CO structure appears at 1900-2200 cm^{-1}, and for M – CO – M structure, it appears at 1750-1900 cm^{-1}. Although in recent years ^{13}C-NMR spectroscopy has become increasingly valuable, it is still true that infrared (IR) spectroscopy is the preeminent physical method for characterizing metal-carbonyls.[21]

To examine the electronic structure of an organometallic compound and to study its redox behavior, electrochemical methods are applied. Electrochemistry is that branch of chemical analysis that employs electrochemical methods to obtain information related to the amounts, properties, and environments of chemical

species.[22] Among the electrochemical methods, cyclic voltammetry, CV, is the most suitable in determining both the oxidation state and the redox behavior of the organometallic compound in question. Cyclic voltammetry is the voltammetric technique in which the current that flows in a system is measured and the potential is changed as a linear function of time.[23]

A full band detailed understanding of the electron transfer properties of organometallic complexes can be achieved only by a combination of spectroscopic and electrochemical studies. For example, the combination of UV-Visible electronic absorption spectroscopy and cyclic voltammetry can provide additional useful information about the electronic structure of the organometallic compounds. [24] Spectroelectrochemistry refers to this kind of techniques, in which a spectroscopic probe is used to monitor electrochemical events in-situ with intimate coupling of the electrochemical and spectroscopic processes. The optical and electrochemical measurements are made simultaneously and the results include quantitative, qualitative, and dynamic information about species involved in the electrochemical reaction.[25]

The aim of this study is to synthesize Group 6 metal-carbonyl complexes of a ferrocene functionalized imine ligand which would have at least long-range metal-metal interaction through π-conjugation. N,N'-bis(ferrocenylmethylene)ethylenediamine appears to be a suitable ligand to form complexes of this kind. N,N'-bis(ferrocenylmethylene)ethylenediamine has two potentially nitrogen atoms, of which is in conjugation with, the cyclopentadienyl ring of a ferrocenyl moiety (Figure 1.2). The N,N'-bis(ferrocenylmethylene)ethylenediamine has already been isolated,[26] but its coordination behavior has not been intensively described. To date, only some zinc, copper, iron complexes have been reported.[27] The complexes with the Group 6 metals are not known. In this study, we report the synthesis, characterization of tetracarbonyl[N,N'-bis(ferrocenylmethylene)ethylenediamine]chromium(0). The

complex could be isolated from the ligand substitution of $Cr(CO)_4(\eta^{2:2}$-1,5-cyclopentadiene) with N,N'-bis(ferrocenylmethylene)ethylenediamine and fully characterized by IR, MS, NMR spectroscopic techniques (Figure 1.3).

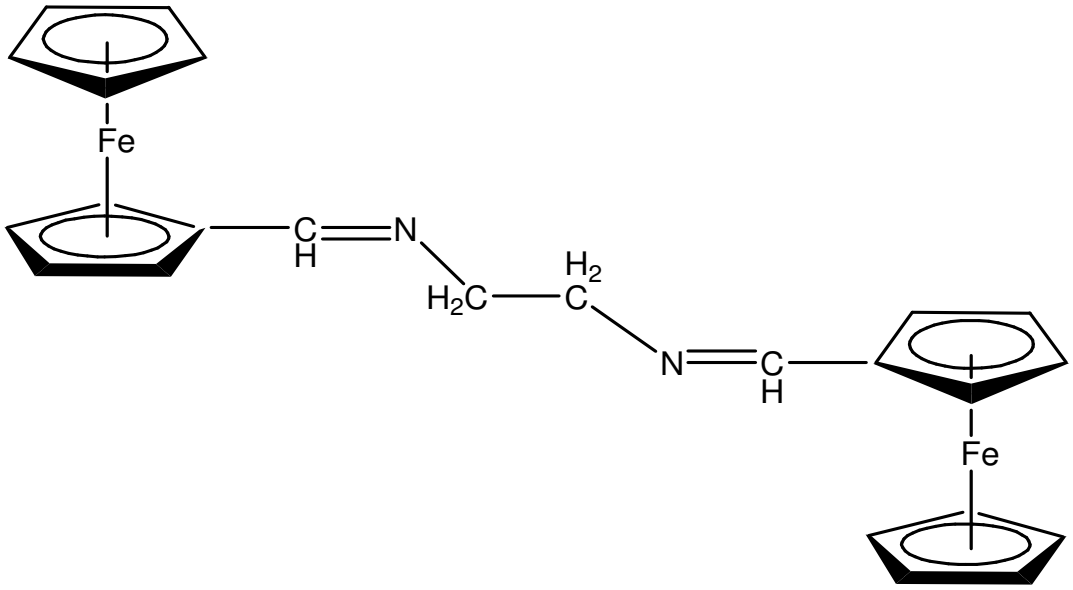

Figure 1.2. Suggested structural formula of BFEDA

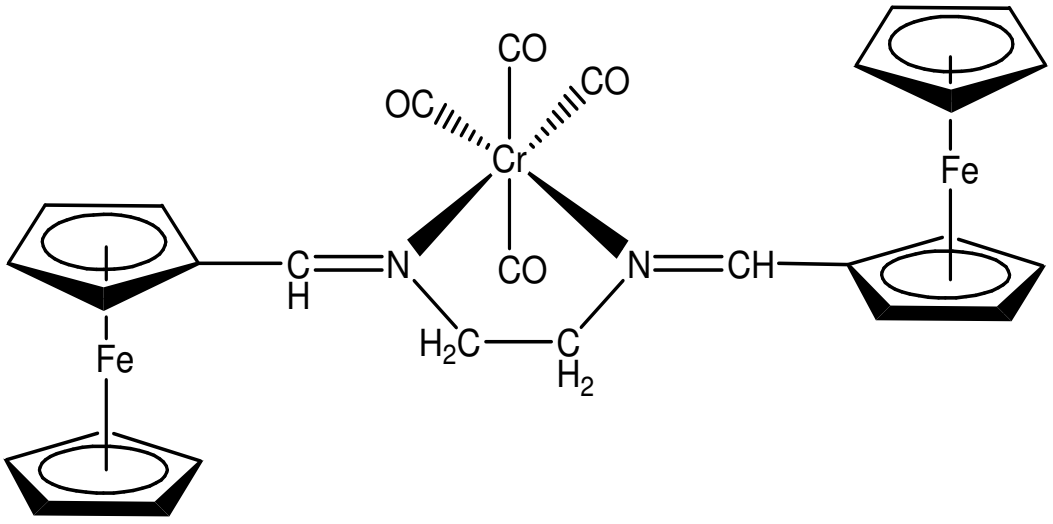

Figure 1.3. Suggested structural formula of $Cr(CO)_4$(BFEDA)

CHAPTER 2

BONDING

2.1. Carbonyl Complexes and Metal-Carbonyl Bonding

Carbonyl complexes are compounds that contain carbon monoxide as a coordinated ligand. Carbon monoxide is a common ligand in transition metal chemistry, in part due to the synergistic nature of its bonding to transition metals. We can describe the bonding of CO to a metal as consisting of two components. The first component is a two electron donation of the lone pair on carbon (coordination exclusively through the oxygen is extremely rare) into a vacant metal d-orbital. This electron donation makes the metal more electron rich, and in order to compensate for this increased electron density, a filled metal d-orbital may interact with the empty π^*-orbital on the carbonyl ligand to relieve the added electron density. This second component is called π-backbonding or π-backdonation. This is shown diagrammatically as well as through a simple MO picture in Figure 2.1.1.

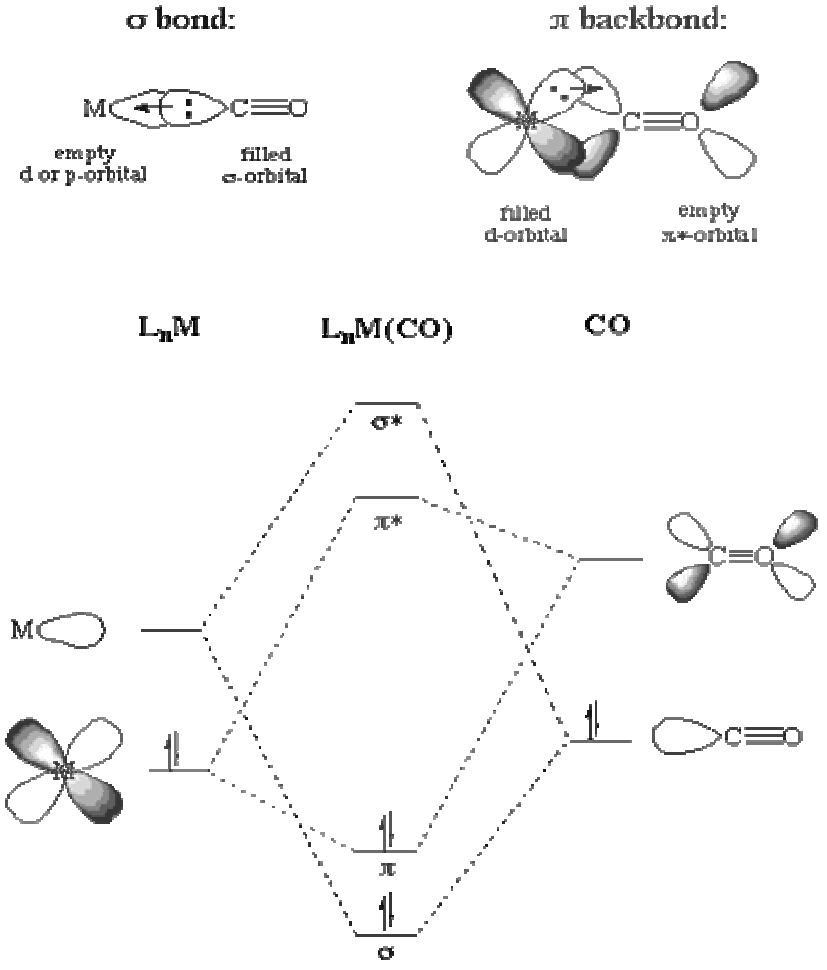

Figure 2.1.1. Part of a molecular orbital diagram of a ML_nCO complex

The two components of this bonding are synergic: The more sigma donation by the carbonyl (or other sigma-donors on the metal center), the stronger the π-backbonding interaction. Notice that although this involves the occupation of a π* orbital on the CO, it is still a bonding interaction as far as the metal center is concerned. This occupation of the π* on CO does lead to a decreased bond order in the carbon monoxide molecule itself. As the π-backdonation becomes stronger, the CO bond order should decrease from that of the free ligand. Two consequences might be expected, if the CO bond order was reduced: 1. lengthening of the C-O bond and 2. a decrease in the carbonyl stretching frequency in the IR.[28]

2.2. Metal-Imine Bonding

Aldehydes or ketones react with primary amines (RNH_2) to form compounds with a carbon–nitrogen double bond are called imines (RCH=NR or R_2C=NR). The product can form as a mixture of (E) and (Z) isomers. The most important step in this reaction is the formation of water, as it might cause a back-reaction.[29]

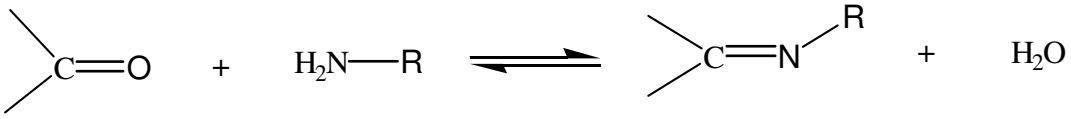

The carbon-nitrogen double bond in an imine molecule consists of a σ bond and a π bond. In the MO energy level diagram (Figure 2.2.1) there will be two σ orbitals (bonding and antibonding) and two π orbitals (bonding and antibonding) for C=N: moiety. The bonding orbitals are mainly localized on the nitrogen atom, while antibonding orbitals belong mainly on the carbon atom, considering the fact that nitrogen is more electronegative than carbon. The HOMO of the imine molecule is the nonbonding σ-orbital, and the LUMO is the antibonding π^*-orbital. A strong σ interaction between metal and the imine ligand should be expected because the HOMO is directed to the dσ-orbital of the metal along the bond-axis (Figure 2.2.2.a). However, the π-bonding takes place to the lower extent in comparison with the σ-bonding because the π^*-orbital (LUMO) of imine is mainly localized on the carbon atom, that is, the LUMO has its smaller amplitude on the nitrogen (Figure 2.2.2.b).[19]

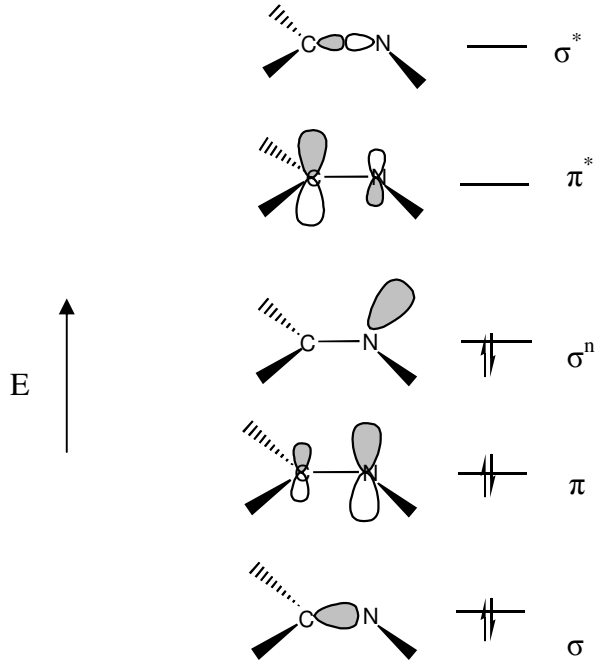

Figure 2.2.1. The molecular orbital diagram of an imine molecule

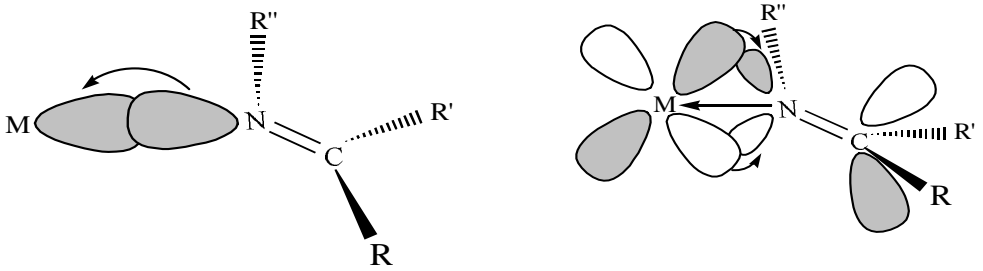

Figure 2.2.2. Molecular orbital description of the metal-imine bonding;

(a) Metal ← imine σ-bonding;

(b) Metal → imine π-bonding.

CHAPTER 3

EXPERIMENTAL

3.1. Basic Techniques

Most of the organometallic compounds are air sensitive and tend to decompose if not handled properly. Those compounds can be oxidized easily, especially when they are in solution, because of their sensitivity to oxygen and water. Consequently, handling and all reactions of organometallic compounds should be carried out under dry and deoxygenated atmosphere or under vacuum.

In order to achieve such an atmosphere, an inert gas line, in which oxygen-free dry dinitrogen passes, have been used. Circulated nitrogen gas passes through some purification steps as shown in Figure 3.1.1. First, nitrogen gas passes through a catalyst (BASF R3.II, Ludwigshafen, Germany) which is heated up to 120°C to remove oxygen and then through dried molecular sieves to remove its moisture and finally through glycerine to bubble the flowing gas.

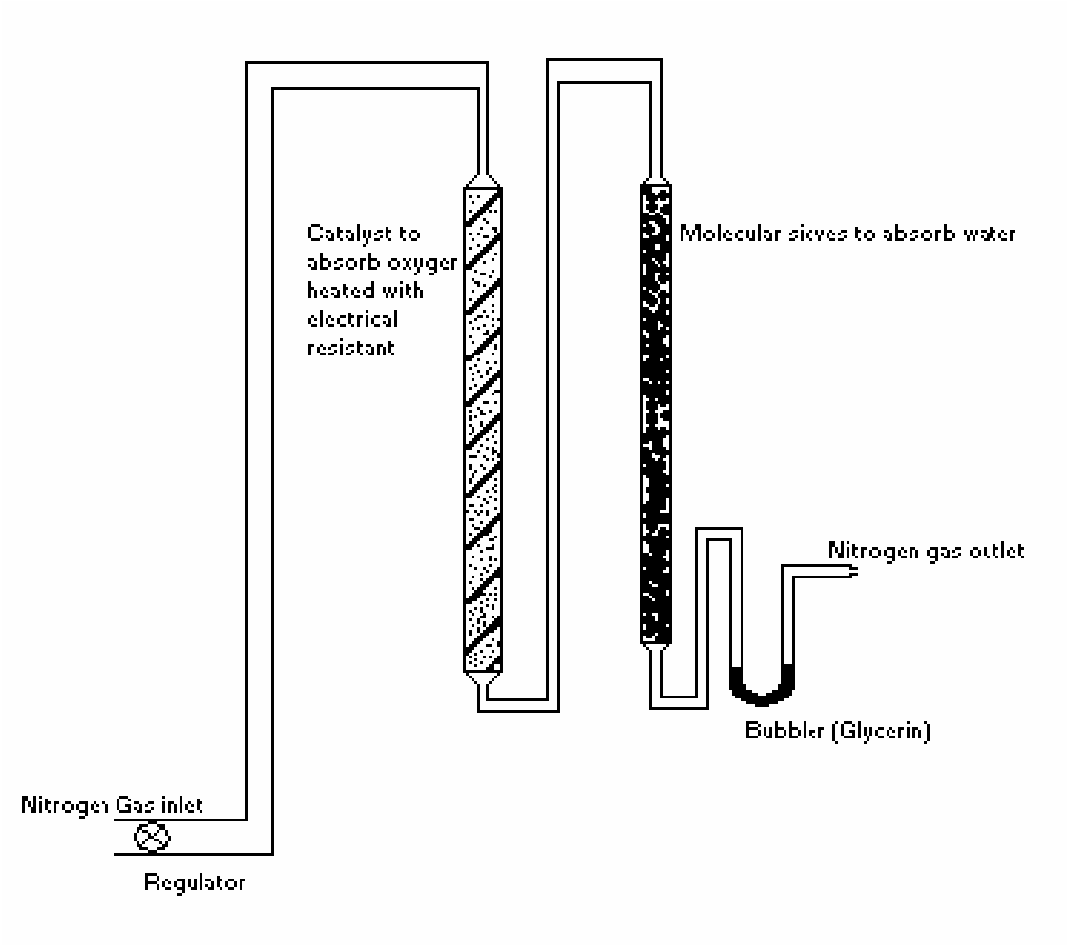

Figure 3.1.1. Nitrogen gas purification steps

Solvents used were purified and the dissolved oxygen was removed by refluxing over sodium or phosphorus pentaoxide under nitrogen atmosphere for 3 to 4 days before use.

The other fundamental techniques that are used in this study are:

(i) Schlenk Technique: A Schlenk tube (Figure 3.1.2) is a flask that has at least one arm where inert gas can be introduced. Usually a three- or two-way stopcock is fitted at the end of the arm. In use, the air in a Schlenk flask should be replaced at least three times

by an inert gas, using a pump and fill procedure and all subsequent handling should be carried out under nitrogen flow. When liquid is transferred by a syringe, great care should be taken, since solutions are generally much more susceptible to oxidation or hydrolysis.[30]

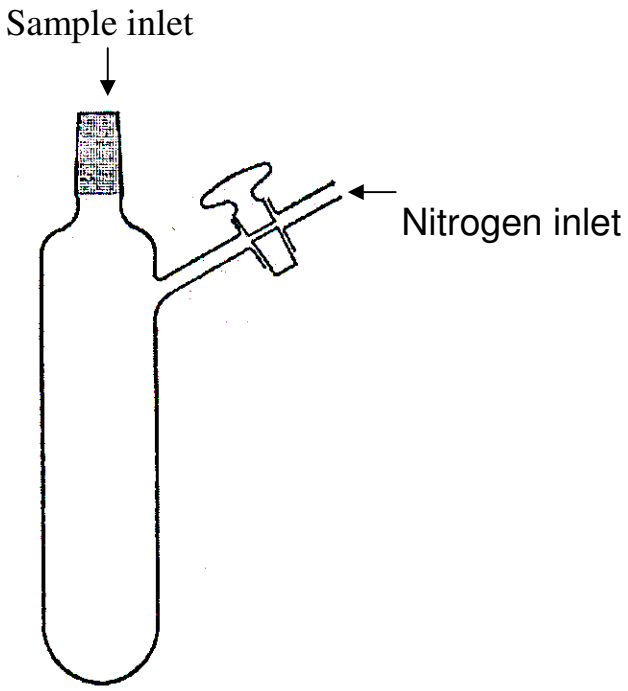

Figure 3.1.2. Standard schlenk tube

(ii) Vacuum Line Technique: This technique is used to remove any solvent under low vapor pressure. The tube used for this technique should be trapped in a dewar vessel containing liquid nitrogen.

All solvents, ferrocenecarboxaldehyde, hexacarbonylchromium were purchased from Aldrich. Ethylenediamine was purchased from Merck.

3.2. Infrared Spectra

The infrared spectra of both the ligand and the complex were recorded from their dichloromethane or toluene solutions by using a Specac IR-Liquid cell with CaF_2 windows on a Nicolet 510 FTIR Spectrometer instrument with Omnic software. The infrared spectrum of the ligand in KBr pellet was also recorded by using a Bruker IFS 66/S Spectrometer with Opus software.

3.3. Raman Spectra

The Raman spectrum of the ligand in solid form was recorded by using a Bruker FRA 106/S Spectrometer with Opus software.

3.4. NMR Spectra

The ^{1}H-NMR and ^{13}C-NMR spectra of the ligand were taken from their d-chloroform solutions on a Bruker-Spectrospin DPX 400 Ultrashield NMR Spectrometer with Avance software in the METU Control Laboratory.

3.5. Mass Spectra

The mass spectrum (MS-FAB) of the complex was taken on a Fisons VG Autospec instrument at Colorado University in USA.

3.6. Elemental Analysis

Elemental analysis was carried by using LECO CHNS-932 instrument in the METU Central Laboratory.

3.7. UV Spectra

The UV-VIS spectra of the ligand and the complex were measured in CH_2Cl_2 solution at room temperature using a Hewlett Packard 8452A Model Diode Array Spectrophotometer with UV-Visible ChemStation software.

3.8. Cyclic Voltammetry

Cyclic Voltammetry studies of the ligand and the complex were performed in CH_2Cl_2 solution using tetrabutylammonium tetrafluoroborate as the electrolyte. An home-made cell (Figure 3.8.1) was used during the CV studies. Ag-wire was used as the reference electrode, whereas the platinum bead electrode and platinum disc electrode were used as working and counter electrodes, respectively. In order to avoid the interference of the reduction waves of oxygen with the waves obtained from compounds, argon gas is allowed to pass through solution before recording. HEKA IEEE 488 model potensiostat was used to record voltammetric measurements.

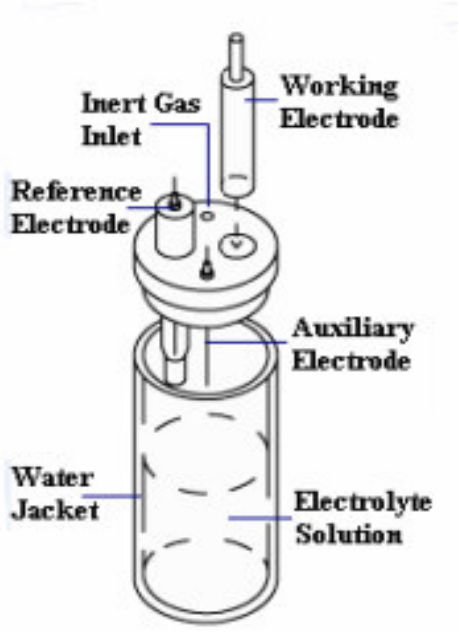

Figure 3.8.1. Cyclic voltammetry cell

3.9. *In-Situ* Constant Potential Electrolysis

Oxidation and reduction processes of the ligand and the complex were carried out at 0°C in their CH_2Cl_2 solution at the peak potentials observed in cyclic voltammetry in a cell shown in Figure 3.9.1. Changes in the electronic absorption spectra were followed in every 5 mC by using a Hewlett Packard 8453A Model Diode Array Spectrophotometer.

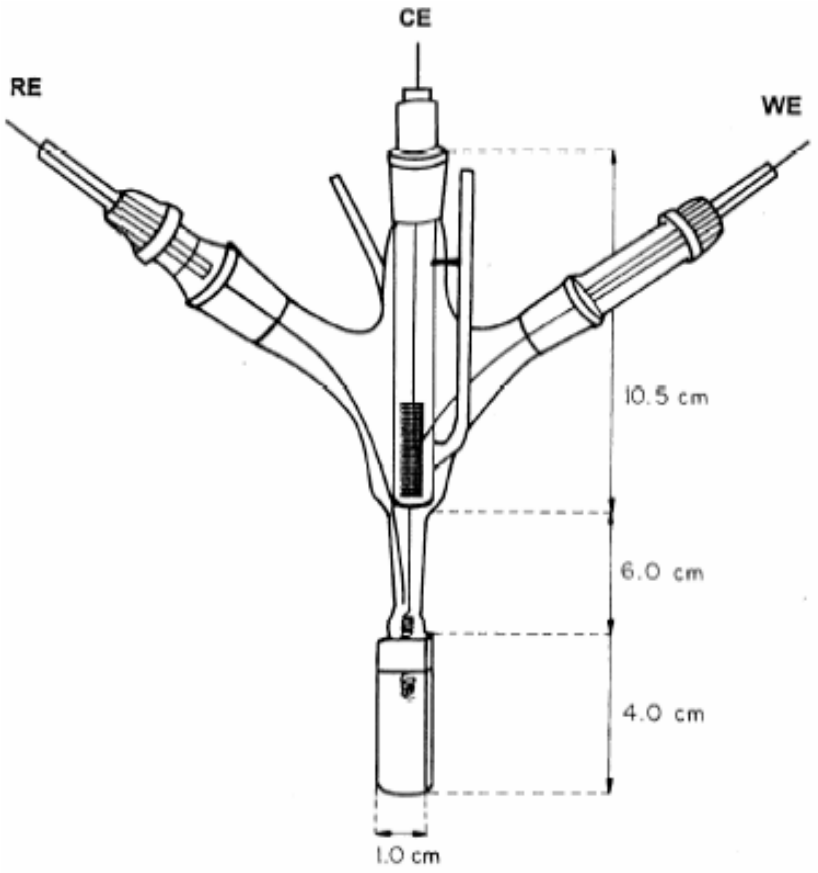

Figure 3.9.1. The cell used for measuring *in-situ* spectral changes during the constant potential electrolysis at room temperature; RE: Ag-wire reference electrode; CE: Pt-sieve counter electrode; WE: Pt-wire working electrode.

3.10. *In-Situ* Constant Current Electrolysis

Oxidation process of the complex was carried out in CH_2Cl_2 at a constant current by using an home-made constant current supplier. The cell used during *in-situ* constant current electrolysis is shown in Figure 3.10.1. Changes in the infrared spectra were followed in every 1 mC by using a Nicolet 510 FTIR Spectrometer with Omnic software.

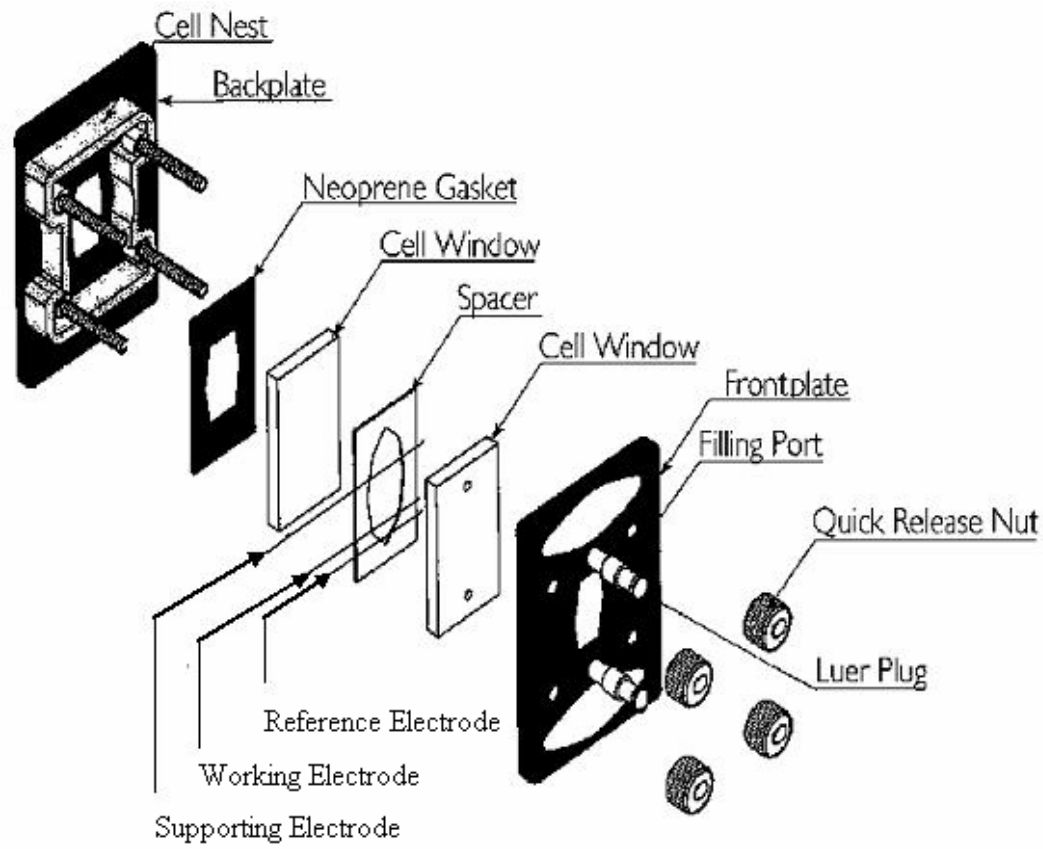

Figure 3.10.1. The cell used for measuring *in-situ* spectral changes during the constant current electrolysis at room temperature; Reference Electrode: Ag-wire reference electrode; Supporting Electrode: Pt-sieve counter electrode; Working Electrode: Pt-wire working electrode.

3.11. Syntheses

3.11.1. Synthesis of N,N'-bis(ferrocenylmethylene)ethylenediamine

N,N'-bis(ferrocenylmethylene)ethylenediamine, BFEDA (Figure 3.11.1.1), was prepared by using a procedure similar to the one given in literature for the preparation of similar ferrocenylimines.[31,32] Ferrocenecarboxaldehyde (2.180 g, 10.2 x 10^{-3} mol) was dissolved completely in 30 mL of benzene at room temperature. Then 0.306 g (5.1 x 10^{-3} mol) of ethylenediamine was added. The flask containing the reaction mixture was connected to a condenser equipped with a Dean-Stark apparatus (Figure 3.11.1.2) (10 cm^3). The mixture was refluxed for 5 hours in a glycerine bath. The hot solution was filtered. After cooling down to room temperature, the solution was dried in a rotary evaporator yielding a yellow precipitate. The residue was dissolved in 10 mL of CH_2Cl_2. The solution was cooled down to -35 ºC. During this period, yellow crystals formed. After decantation of the mother liquour the crystals were dried in vacuum. Percent yield of the BFEDA is 91%. IR (CH_2Cl_2) ν(C=N)=1646 cm^{-1}; UV-VIS (CH_2Cl_2) λ(CT) = 230 nm (ε = 2.965 x 10^4 L/mol.cm) and 274 nm (ε = 1.650 x 10^4 L/mol.cm), λ(d-d)= 330 (ε = 0.275 x 10^4 L/mol.cm) and 460 nm (ε= 0.105 x 10^4 L/mol.cm); ^{1}H-NMR ($CDCl_3$) δ = 8.2 (-C**H**=N-), 3.6 (-C**H_2**), 4.1 (C_5**H_5**), 4.3 (**H3** and **H4** of C_5H_4) and 4.6 (**H2** and **H5** of C_5H_4) ppm; ^{13}C-NMR ($CDCl_3$) δ = 162.661 (-**C**=N-) ppm; CV(CH_2Cl_2) Ox. Pot. = 0.567V, Red. Pot. = 0.462V.

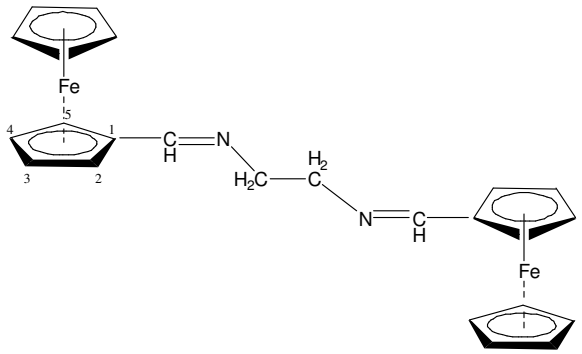

Figure 3.11.1.1. Suggested structure of BFEDA

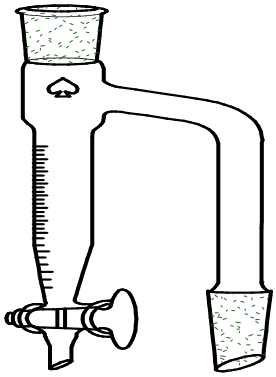

Figure 3.10.1.2. Dean-Stark Apparatus

3.11.2. Synthesis of the $Cr(CO)_4(\eta^{2:2}$-1,5-cyclooctadiene)

Tetracarbonyl($\eta^{2:2}$-1,5-cyclooctadiene)-chromium(0), $Cr(CO)_4(\eta^{2:2}$-COD), was prepared by irradiation of hexacarbonylmetal(0) and COD in n-hexane at room temperature using a procedure described in literature.[33] When all hexacarbonylmetal(0) was consumed, as monitored by IR, the mixture was filtered to remove colloidal decomposition products. The solvent and excess COD were removed under reduced pressure. The residue was dissolved in n-hexane and the solution was allowed to stand for 1 day at -35 °C for crystallization. The solvent was decanted and crystals were dried in vacuo.[34] IR (toluene) ($A_{1(2)}$) = 2022, ($A_{1(1)}$) = 1924, (B_1) = 1940, (B_2) = 1883 cm^{-1}.

3.11.3. Synthesis of Tetracarbonyl[N,N'-bis(ferrocenylmethylene) ethylenediamine]chromium(0), $Cr(CO)_4$(BFEDA)

A quantity of 0.100 g (0.365 mmol) of $Cr(CO)_4(\eta^{2:2}$-COD) was dissolved in 15 mL of toluene in a jacketed schlenk. Then 0.113 g (0.25 mmol) of BFEDA was added to the above solution with stirring at 38 °C. The mixture was stirred for two hours with a magnetic stirrer. When the ligand exchange reaction was over, as monitored by taking the IR spectra, the solution was brought to dryness under vacuum. The solid part was then washed with n-hexane in order to remove any unreacted $Cr(CO)_4(\eta^{2:2}$-COD), COD evolved, and other impurities. The remaining yellow precipitate was dissolved in 1:1 CH_2Cl_2/toluene solution for recrystallization. Yellow, needle like crystals of $Cr(CO)_4$(BFEDA) (Figure 3.11.3.1) were obtained when left at -35 ºC for 2 days. The crystals were dried in vacuum. Percent yield is 62%. Analyses: Calculated for $C_{28}H_{24}O_4N_2Fe_2Cr$: C, 54.5; H, 5.2; N, 4.0; Found: C, 54.9; H, 3.9; N, 4.0; IR (CH_2Cl_2) $\nu_{C=O}$: 2004, 1887, 1870, 1822; $\nu_{C=N}$: 1620, 1606 cm^{-1}. UV-VIS (CH_2Cl_2) λ(CT)= 233 nm ($\varepsilon = 3.915 \times 10^4$ L/mol.cm) and 269 nm ($\varepsilon = 2.312 \times 10^4$ L/mol.cm), λ(d-d)= 340 nm ($\varepsilon = 0.623 \times 10^4$ L/mol.cm) and 450 nm ($\varepsilon = 0.265 \times 10^4$ L/mol.cm); Molecular peak (m/z) = 616; CV(CH_2Cl_2) Ox. Pot. = 0.263, 0.610, 0.765V, Red. Pot. = 0.561V. ; ^{1}H-NMR (CD_2Cl_2) δ = 8.503 (-C**H**=N-), 3.666 (-C**H_2**), 4.258 (C_5**H_5**), 4.588 (**H3** and **H4** of C_5H_4) and 5.091 (**H2** and **H5** of C_5H_4) ppm; ^{13}C-NMR (CD_2Cl_2) δ = 171.070 (-**C**=N-) ppm, 217.330, 228.513 (**C**O), 78.296 (**C1** of C_5H_4), 72.304 (**C3** and **C4** of C_5H_4), 72.504 (**C2** and **C5** of C_5H_4), 70.082 (**C_5**H_5), 66.130 (**C**H_2).

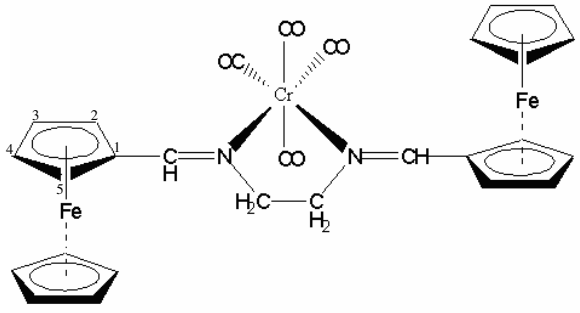

Figure 3.11.3.1. Suggested structure of $Cr(CO)_4$(BFEDA)

CHAPTER 4

RESULTS AND DISCUSSION

4.1. Synthesis and Characterization of BFEDA

Synthesis of BFEDA was carried out according to a procedure that is used for most of ferrocenylimines.[31,32] In this method ferrocenecarboxaldehyde and the corresponding amine are refluxed in benzene using a Dean-Stark apparatus, which is used in order to hold benzene-water azeotrope away from the reaction mixture. The condensation reaction (Scheme 4.1.1) was followed by taking IR spectra from the reaction solution. In the IR spectrum, it was observed that as the peak at 1685 cm^{-1} corresponding to aldehyde decreased, a new peak at 1645 cm^{-1} corresponding to imine formation increased. When the reaction was completed after five hours, the solution was cooled down and the volatiles were removed in a rotary-evaporator. The residue was dissolved in dichloromethane and crystallized at -35 ºC.

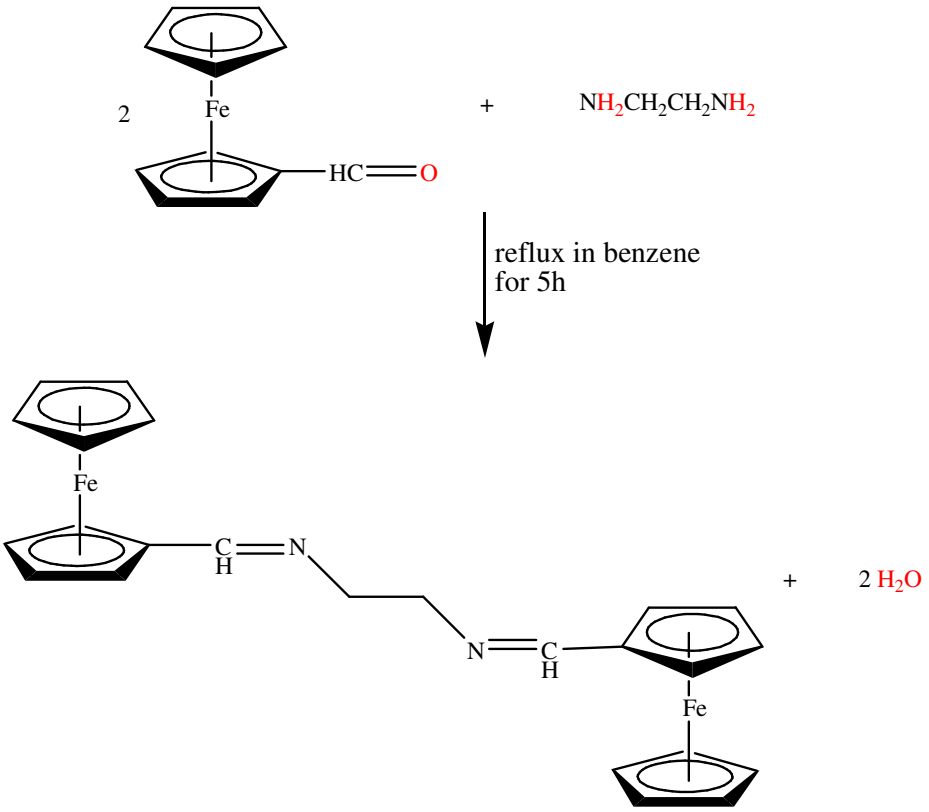

Scheme 4.1.1. Formation reaction of BFEDA

N,N'-bis(ferrocenylmethylene)ethylenediamine was obtained as yellow crystals and characterized by using IR, Raman, UV-VIS and NMR spectroscopy techniques. IR spectrum which is taken in CH_2Cl_2 solution (Figure 4.1.1) gives a sharp peak at 1645 cm^{-1} indicating the stretching of the –C=N– group. The ^{1}H-NMR (Figure 4.1.5) and ^{13}C-NMR spectra (Figure 4.1.6) give all the expected peaks for BFEDA. In ^{1}H-NMR spectrum, the peak at 8.2 ppm was assigned to the hydrogen atom of –C**H**=N– group. The peak corresponding to the same group was also observed in ^{13}C-NMR spectrum at 162.673 ppm. These peaks indicating the formation of (– CH=N–) are evidences for the successful synthesis of BFEDA.

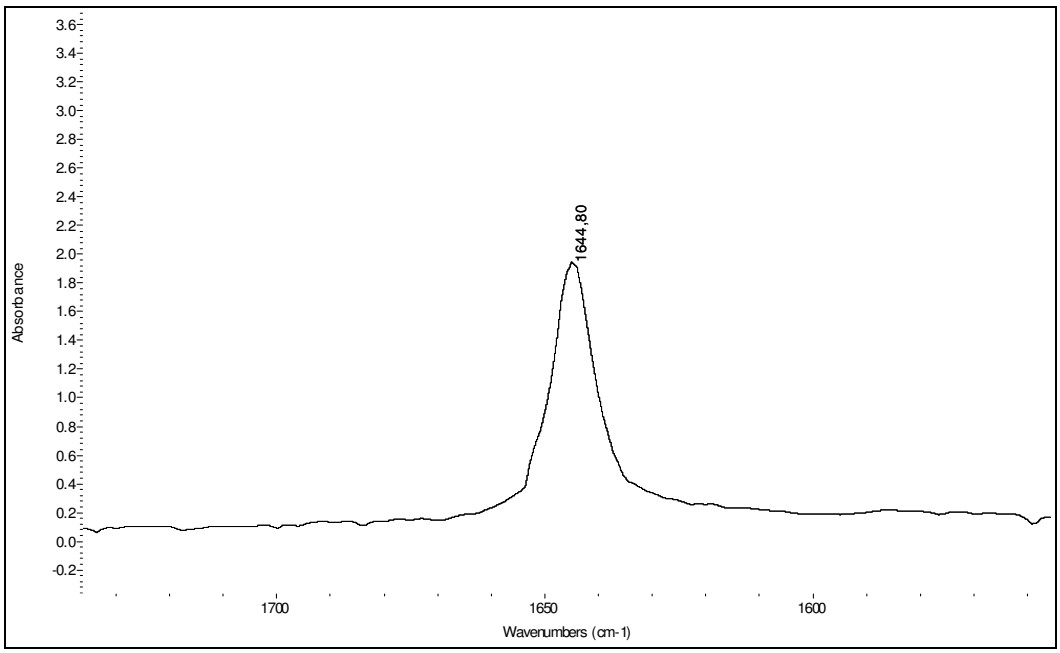

Figure 4.1.1. The IR Spectrum of BFEDA in CH_2Cl_2 at room temperature

The two carbon–nitrogen double bonds in free BFEDA molecule have a zig-zag shape as shown in Figure 4.1.2. Thus, there are two stretching modes: 1. symmetric 2. antisymmetric stretching. While one mode is Raman active, the other should be IR active as this is an instance of a general rule, the Rule of Mutual Exclusion; for a molecule with an inversion center, *i*, no vibration can be active in both spectra.[35] This statement was observed clearly in free BFEDA molecule; IR and Raman spectra each gives a single absorption band at 1640 and 1644 cm^{-1} for symmetric and antisymmetric C=N stretching modes, respectively (Figure 4.1.3 and 4.1.4).

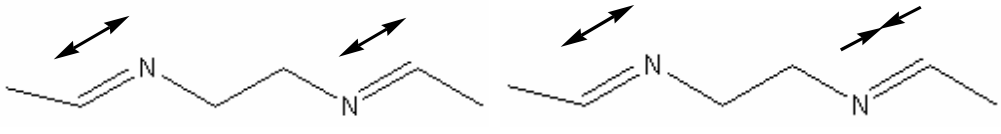

(a) **(b)**

Figure 4.1.2. Representation of stretching modes in BFEDA

(a) Symmetric stretching, (b) Antisymmetric stretching

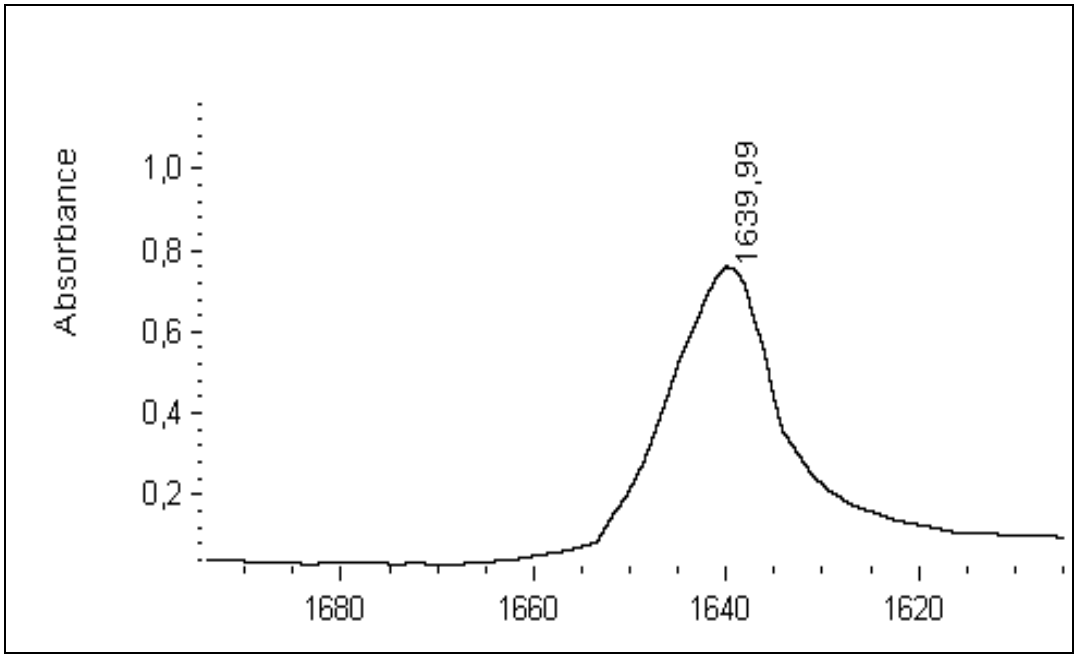

Figure 4.1.3. Infrared spectrum of BFEDA in solid form (KBr pellet)

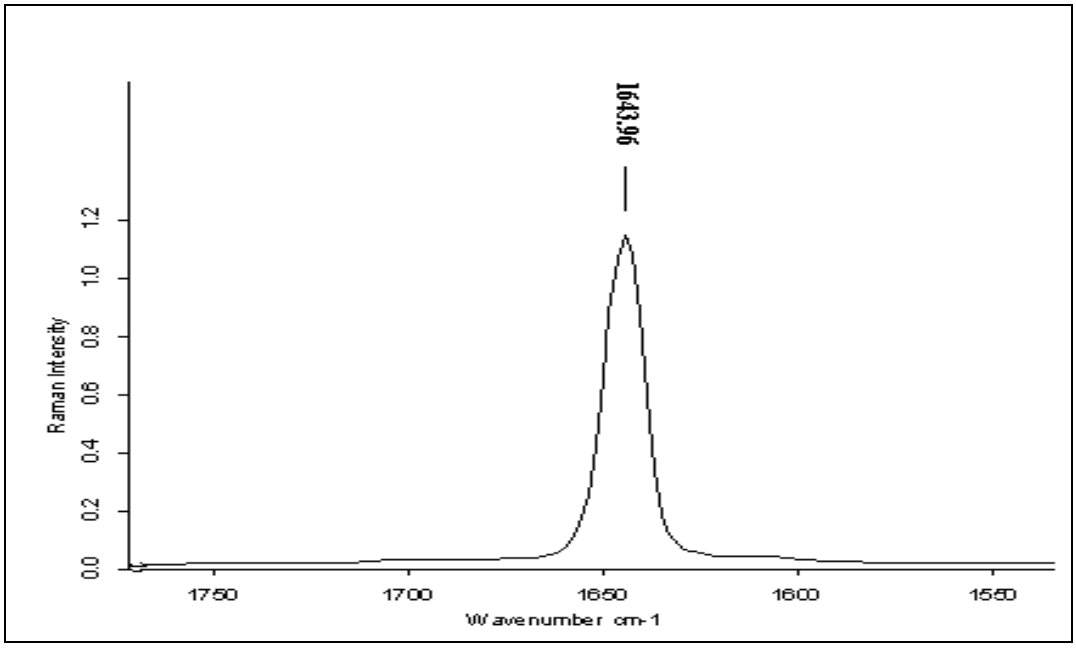

Figure 4.1.4. Raman spectrum of the BFEDA in solid form

The ^{1}H-NMR spectrum of BFEDA (Figure 4.1.5) shows the characteristic ferrocenyl pattern with a singlet at 4.1 ppm for the five equivalent hydrogens of the unsubstituted cyclopentadienyl ring and two singlets at 4.3 and 4.6 ppm for the four hydrogens of the monosubstituted cyclopentadienyl ring with an intensity ratio of 5:2:2, respectively. Observing the latter two peaks as singlets is due to the small coupling between them. As expected for ferrocenyl compounds containing electron-withdrawing substituents, protons of the substituted ring are at lower magnetic field than the protons of the unsubstituted ring. Of the hydrogens of the monosubstituted ring, the closer ones to the electron-withdrawing imine moiety should be more deshielded and they are assigned for the peak at 4.6 ppm.[36]

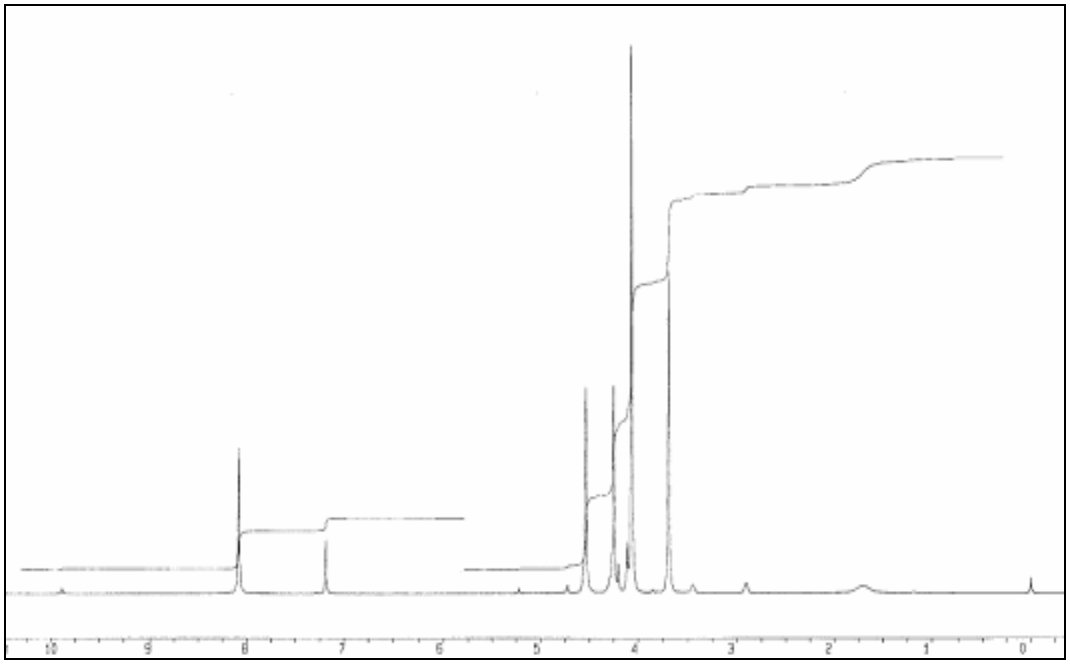

Figure 4.1.5. ^{1}H-NMR Spectrum of BFEDA in $CDCl_3$

The ^{13}C-{^{1}H}-NMR spectrum of BFEDA (Figure 4.1.6) shows three signals at 80.006, 68.833 and 70.711 ppm for the carbons of the substituted cyclopentadienyl ring and one signal at 69.404 ppm for the carbons of the unsubstituted cyclopentadienyl ring with a ratio of 1:2:2:5, respectively. Carbons of the methylene groups of the imine moiety give a signal at 61.538 ppm.

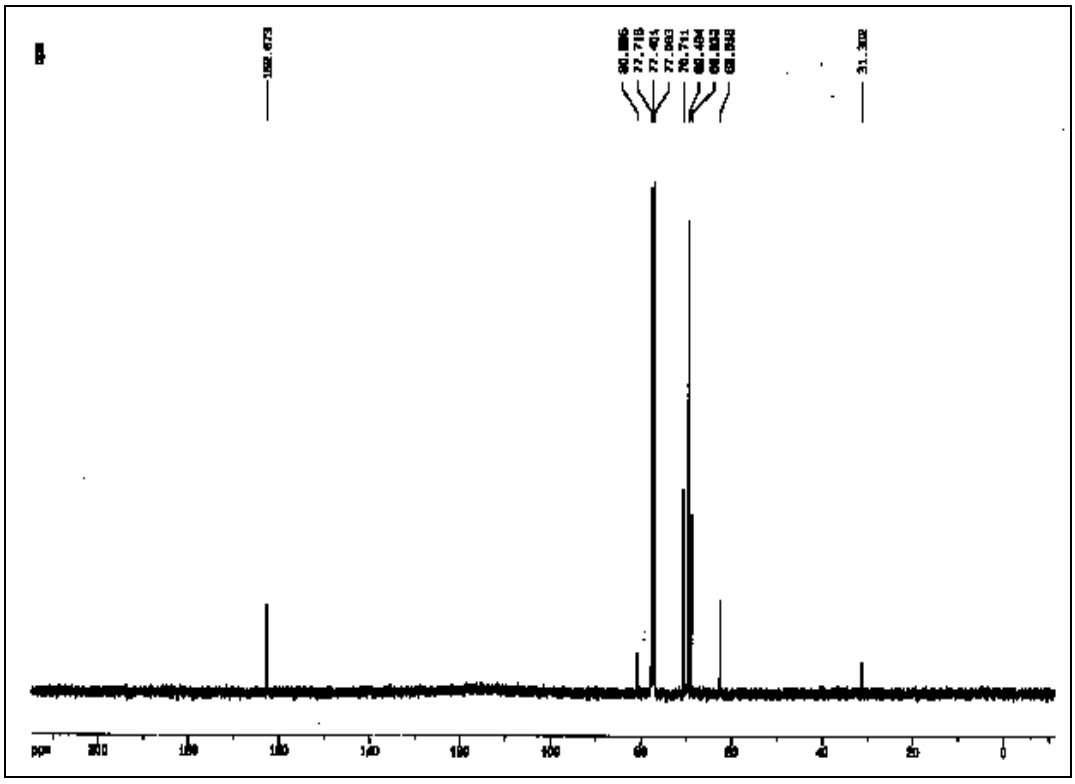

Figure 4.1.6. ^{13}C-{^{1}H}-NMR Spectrum of BFEDA in CD_2Cl_2

In the UV-VIS electronic absorption spectrum of BFEDA (Figure 4.1.7), two absorption bands at 230 and 274 nm are observed. The absorption bands at 230 nm and 274 nm are assigned to the charge transfer transition whereas two low-intensity bands at 330 and 460 nm are attributed to d-d transitions.[37]

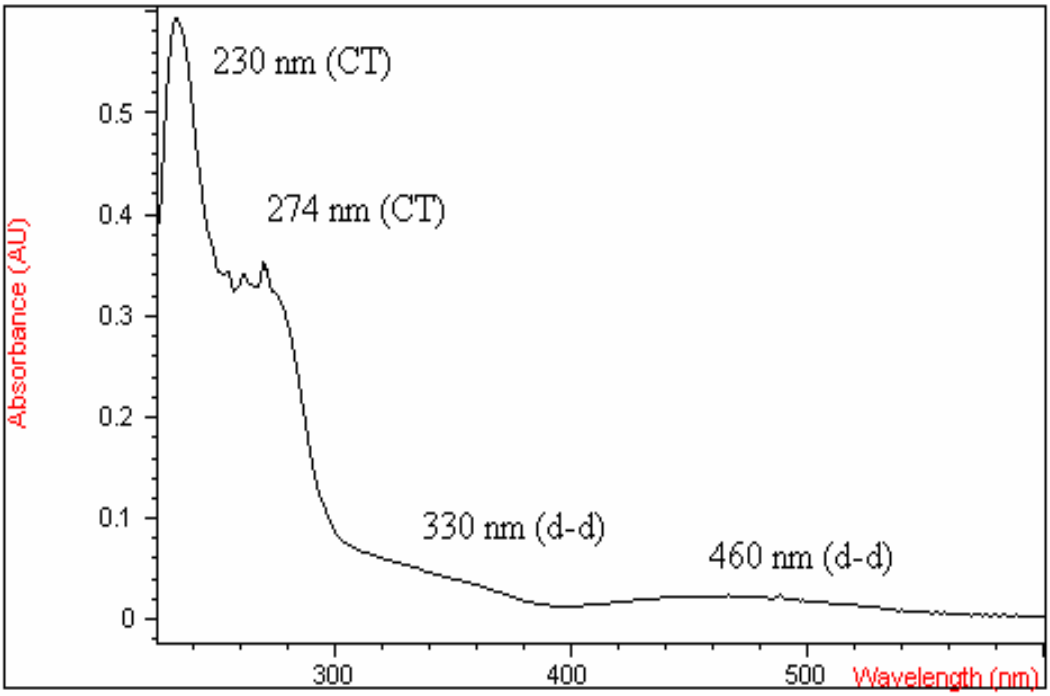

Figure 4.1.7. UV-VIS electronic absorption spectrum of BFEDA in CH_2Cl_2 taken at room temperature

Cyclic Voltammogram of BFEDA consists of an oxidation peak at 0.567V, and a reduction peak at 0.462V (Figure 4.1.8). Note that, Ag-wire was used as the reference electrode.

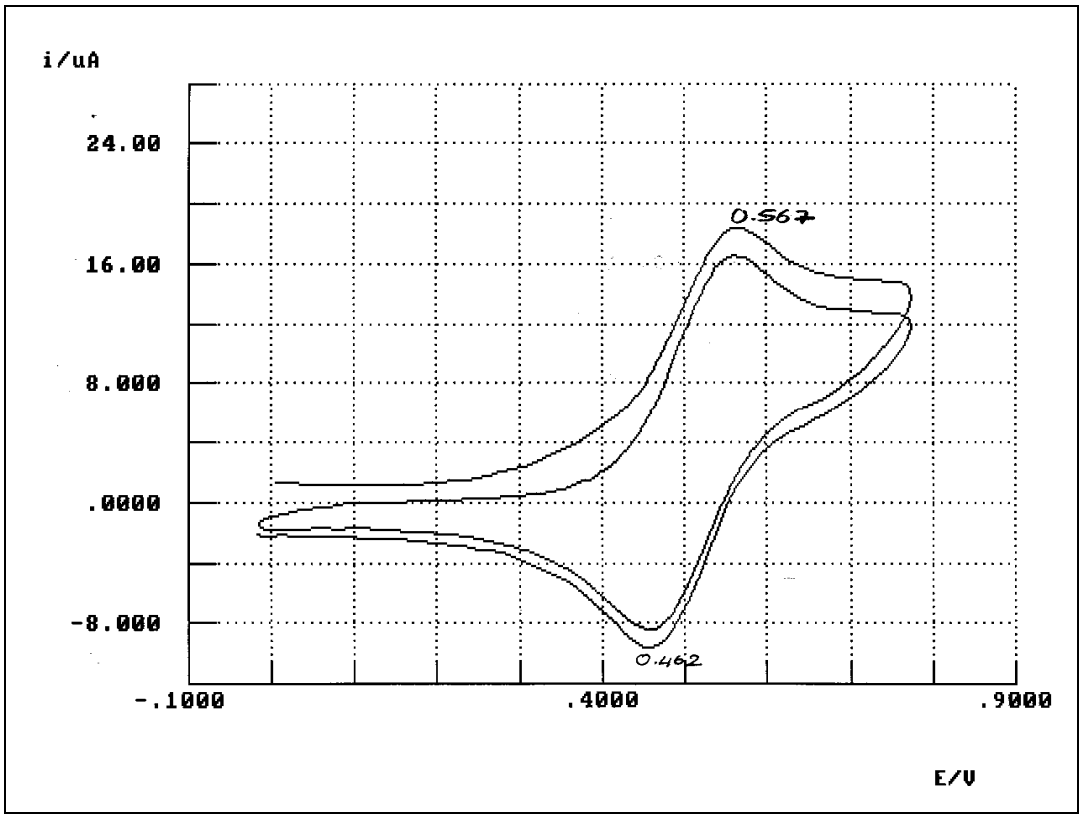

Figure 4.1.8. CV of BFEDA in CH_2Cl_2 solution containing the electrolyte, tetrabutylammonium tetrafluoroborate

The electrochemical oxidation of BFEDA was carried out at the peak potential and the changes in the electronic absorption spectra were followed in-situ by a UV-VIS spectrophotometer (Figure 4.1.9). During the electrochemical oxidation, it was observed that two new shoulders at 268 and 300 nm form. The bands at 330 and 460 nm shift towards lower energies.

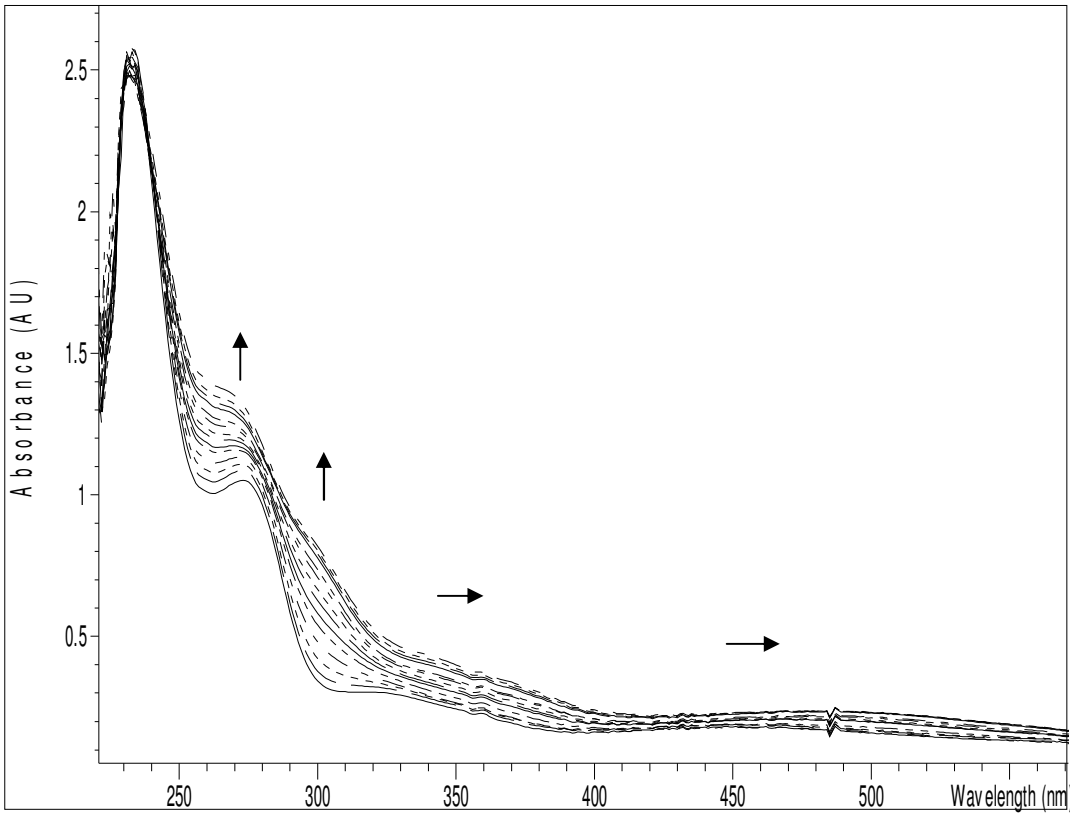

Figure 4.1.9. The UV-VIS electronic absorption spectra of BFEDA recorded during its electrolytic oxidation in CH_2Cl_2 solution containing the electrolyte, tetrabutylammonium tetrafluoroborate

The cyclic voltammogram and spectral changes observed during oxidation are assigned to electron removal from Fe centers in the BFEDA molecule (Scheme 4.1.2).

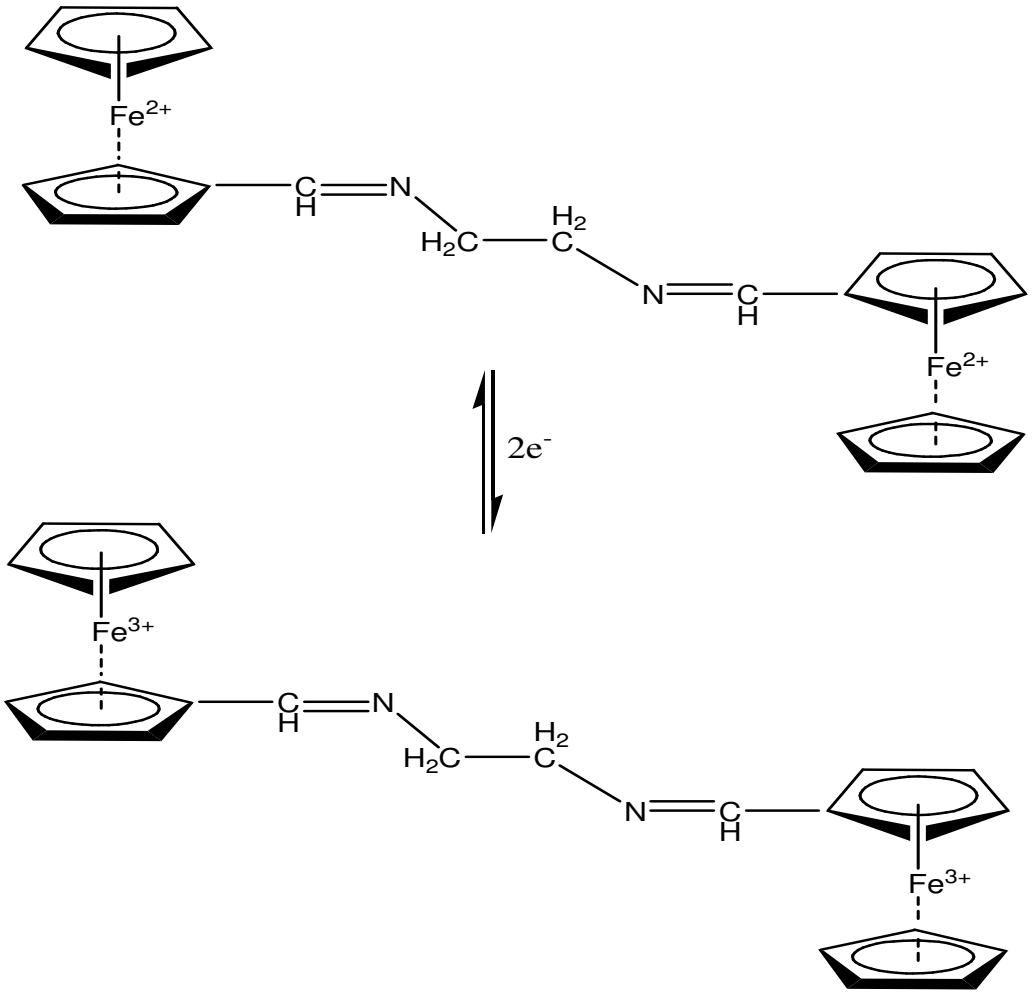

Scheme 4.1.2. Removal of electrons from iron centers in the BFEDA molecule forming ferrocenium cationic centers.

Removal of the electrons from the iron center does not differ from each other. The two iron centers are far away from each other to communicate electronically and there exists no conjugation between them. This is evidenced by observing only one oxidation peak for the two ferrocenyl moieties in the cyclic voltammogram of the BFEDA molecule.

4.2. Synthesis and Characterization of $Cr(CO)_4$(BFEDA)

The complex, $Cr(CO)_4$(BFEDA), was first tried to be synthesized photochemically. However, the photolysis of hexacarbonylchromium(0) in the presence of BFEDA gives the monosubstitution product $Cr(CO)_5$(BFEDA) prior to the $Cr(CO)_4$(BFEDA) complex, the separation of which could not be achieved.

The photolysis of of hexacarbonylchromium(0) in the presence of BFEDA in n-hexane did not give rise to the formation of substitution product in significant amount because of the insolubility of the BFEDA ligand. After two hours irradiation, only 5 % of $Cr(CO)_6$ is converted to a $Cr(CO)_4$ species as seen in the IR spectrum in Figure 4.2.1.

$$Cr(CO)_6 + \text{BFEDA} \xrightarrow[\text{Hexane}]{h\nu} \text{NO REACTON}$$

The irradiation of $Cr(CO)_6$ in the presence of BFEDA in toluene gives mainly the monosubstitution product. In the IR spectrum taken after 7 hours irradiation, one observes moderately intense absorption bands assigned for the CO stretchings of $Cr(CO)_5$(BFEDA) species (2067, 1925, 1895 cm^{-1}) and weak absorption bands for the CO stretchings of $Cr(CO)_4$(BFEDA) (Figure 4.2.2). These species could not be isolated from the solution.

$$Cr(CO)_6 + \text{BFEDA} \xrightarrow[\text{Toluene}]{h\nu} Cr(CO)_4(\text{BFEDA}) + Cr(CO)_5(\text{BFEDA})$$

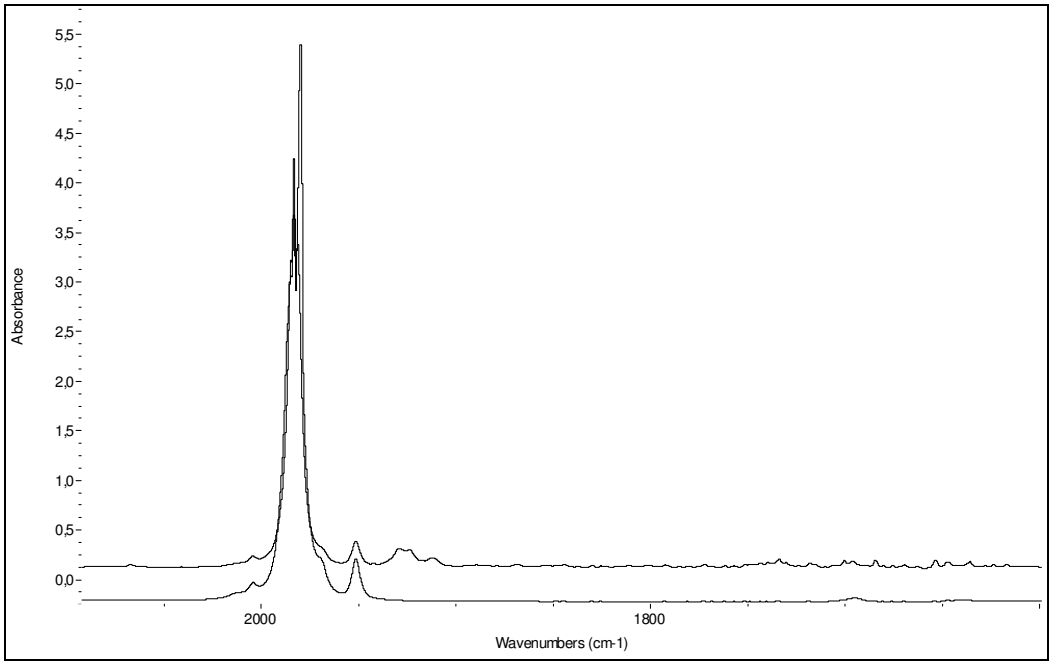

Figure 4.2.1. The IR Spectra at the beginning (spectrum at the bottom) and after 2 hours (spectrum at the top) of the irradiation $Cr(CO)_6$ with BFEDA in n-hexane taken at room temperature

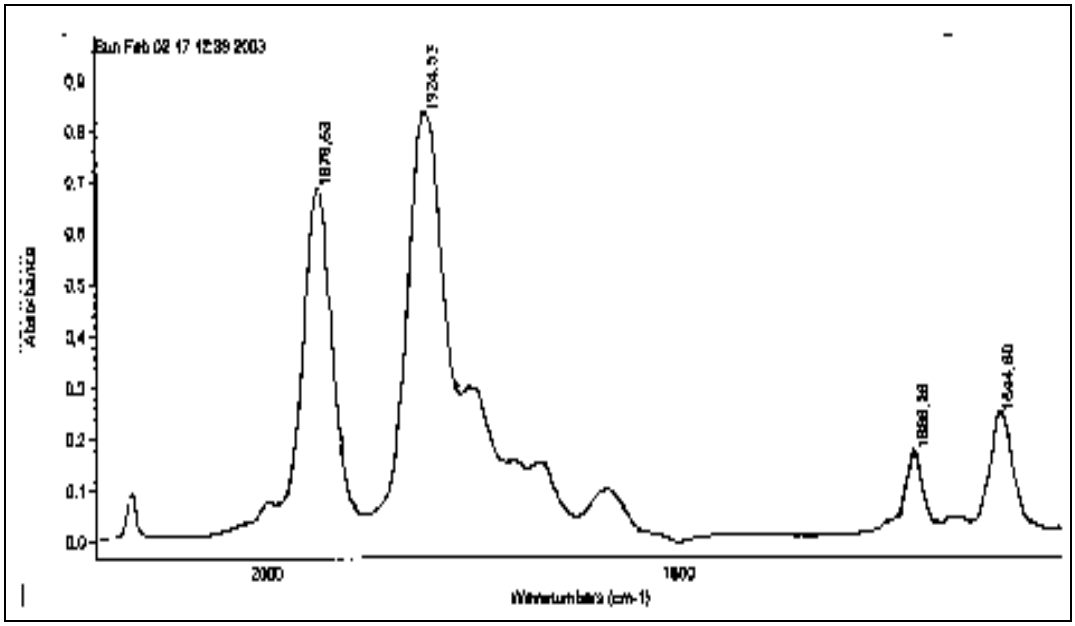

Figure 4.2.2. The IR spectrum taken after seven hours irradiation of $Cr(CO)_6$ with BFEDA in toluene solution

In the second attempt, the thermal substitution of a metastable complex was used to form the $Cr(CO)_4$(BFEDA) complex. Irradiation of hexacarbonylchromium, $Cr(CO)_6$, in THF yields the complex $Cr(CO)_5(THF)$[38] as monitored by taking the FTIR spectra during the photolysis (Figure 4.2.3). The in-*situ* generated complex was then reacted with BFEDA (Figure 4.2.4):

$$Cr(CO)_6 \xrightarrow[THF]{hv} Cr(CO)_5(THF)$$

$$Cr(CO)_5(THF) + BFEDA \longrightarrow Cr(CO)_4(BFEDA) + Cr(CO)_5(BFEDA)$$

However this reaction yields also a mixture of mono- and disubstitution products.

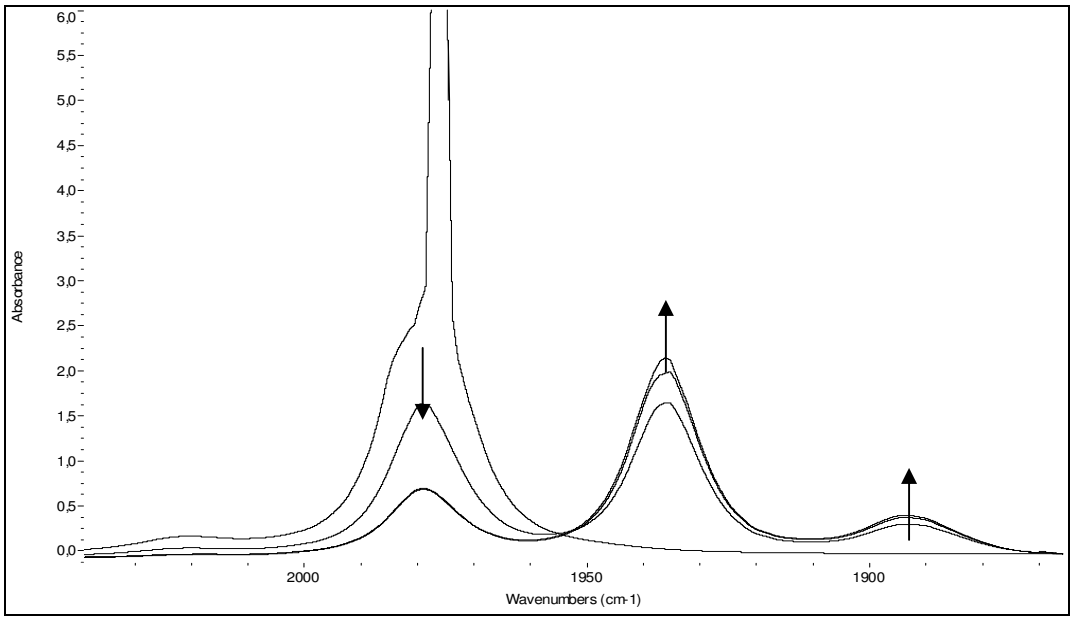

Figure 4.2.3. The IR spectra taken during the **i**rradiation of $Cr(CO)_6$ in THF solution to form $Cr(CO)_5(THF)$

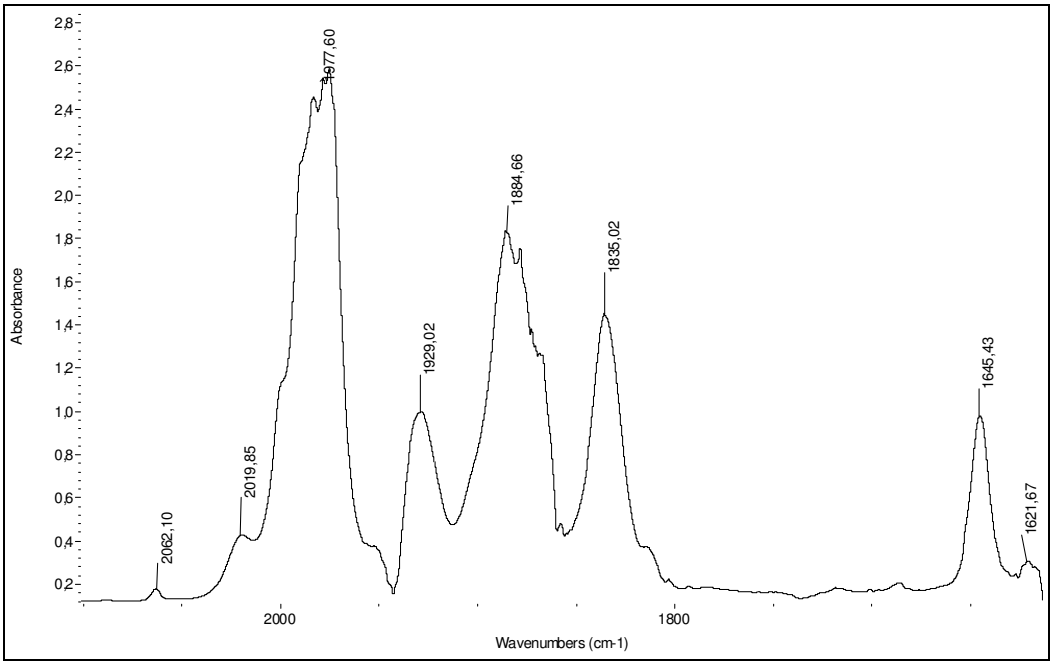

Figure 4.2.4. The IR spectrum taken in toluene after the ligand exchange reaction between $Cr(CO)_5(THF)$ and BFEDA was over

We attempted many methods to purify the $Cr(CO)_4(BFEDA)$ complex including crystallization from the solution in solvents like toluene and dichloromethane at different conditions such as at room temperature, at -35 °C, under dry ice or under liquid nitrogen vapor. Although no crystals were formed after these attempts, we had some precipitates. Separations of the solid part from the liquid part were also tried. Most of these attempts caused in a decrease of the amount of the pentacarbonyl complex (Figure 4.2.5). But, due to long procedures and instability of the complex especially towards air and water, these attempts ended up with decomposition of the complex.

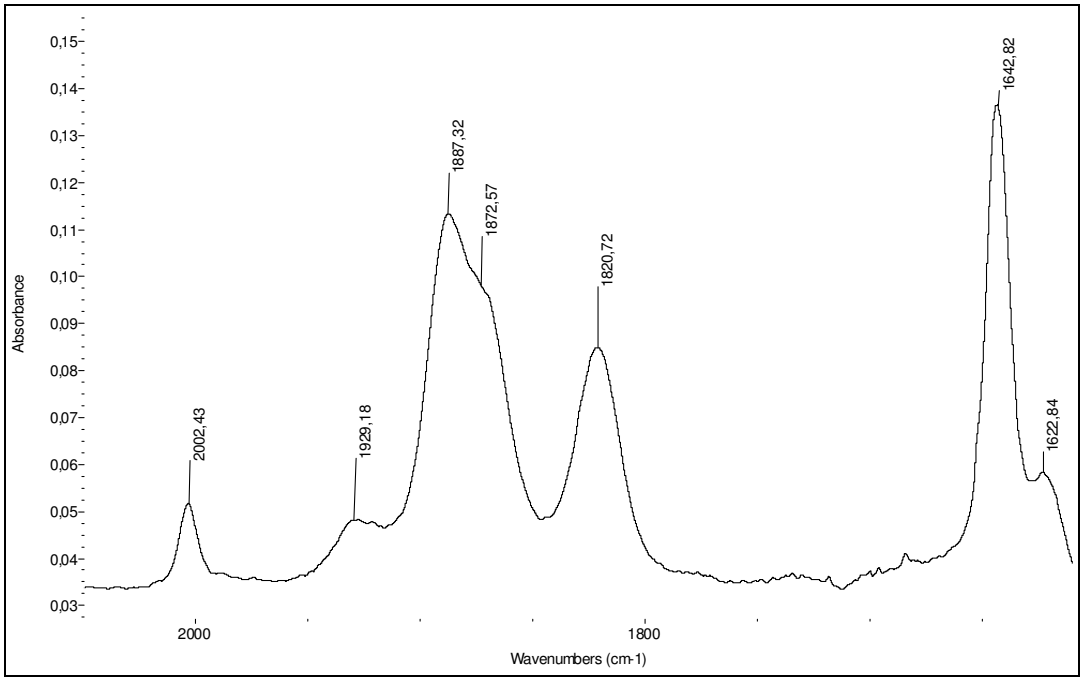

Figure 4.2.5. The IR spectrum taken from the solution containing the $Cr(CO)_4$(BFEDA) complex in CH_2Cl_2 after many purification steps

As most of the organometallic compounds, $Cr(CO)_4$(BFEDA) is also air sensitive and tends to decompose when exposed to air or moisture. In particular, the BFEDA ligand undergoes hydrolysis and converted to the ferocenecarboxaldehyde and ethylenediamine. Upon coordination the imine becomes more prone to the hydrolysis.[19] The π-backbonding from metal to π^*-orbital of the imine weakens the C=N double bond. As a result, this bond becomes very susceptible to be attacked by water to form ferrocenecarboxaldehyde.

As procedures containing photochemical techniques did not succeed and necessity of less number of steps to avoid decomposition, a more direct method have to be found for the synthesis of the $Cr(CO)_4$(BFEDA) complex. This led us to use a $Cr(CO)_4$ transfer reagent, such as tetracarbonyl($\eta^{2:2}$-1,5-cyclooctadiene)chromium(0). The latter complex has already been used as a $Cr(CO)_4$ transfer reagent for the preparation of variety of $Cr(CO)_4L_2$ complexes.[39]

The thermal substitution of 1,5-cyclooctadiene in $Cr(CO)_4(\eta^{2:2}$-COD) with BFEDA at 38 °C yields the $Cr(CO)_4$(BFEDA) complex according to the equation given below:

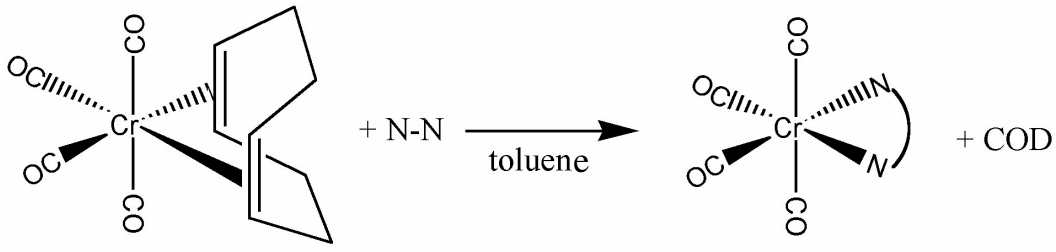

In this equation, COD denotes 1,5-cyclooctadiene and N-N denotes the BFEDA ligand.

The thermal substitution reaction could be followed by taking the FTIR spectra of the reaction solution (Figure 4.2.6 and 7). After the completion of the substitution reaction, the solution was brought to the dryness in vacuum. The residue was redissolved in a 1:1 CH_2Cl_2/toluene mixture. The solution was left at -35 ºC over two days for crystallization. This yielded the needle like yellow crystals of $Cr(CO)_4$(BFEDA). The complex was characterized by means of elemental analysis, IR, ^{1}H-, ^{13}C-{^{1}H}-NMR, UV-VIS and Mass spectroscopy methods. Electrochemical behaviour of the complex was also studied by cyclic voltammetry and the mechanism of electrode reaction was investigated by *in-situ* UV-VIS and IR spectroscopy measurements.

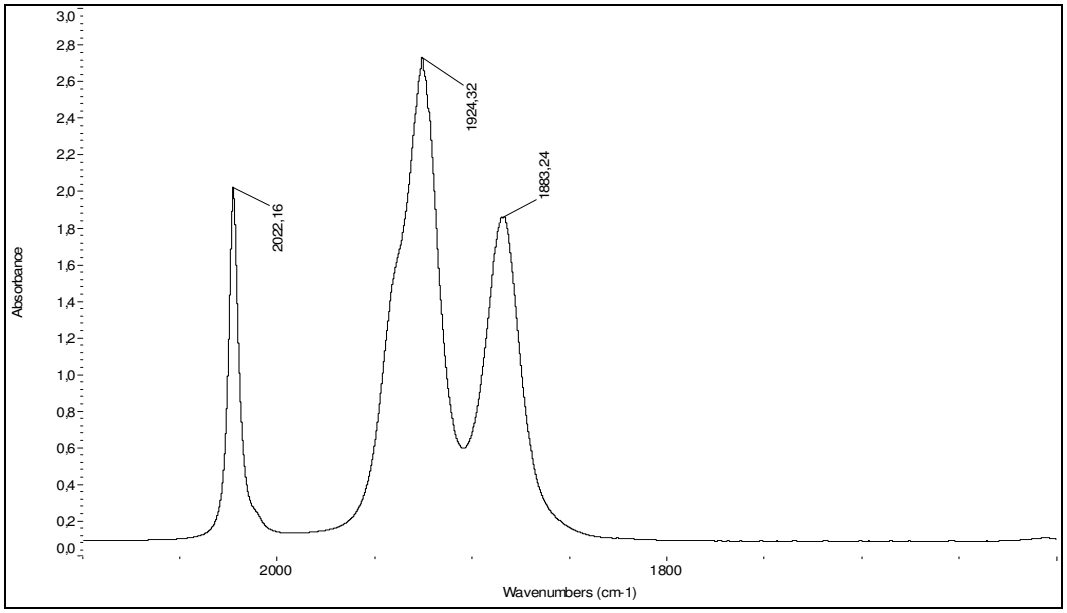

Figure 4.2.6. The IR Spectrum of $Cr(CO)_4(\eta^{2:2}$-COD) in toluene taken at room temperature

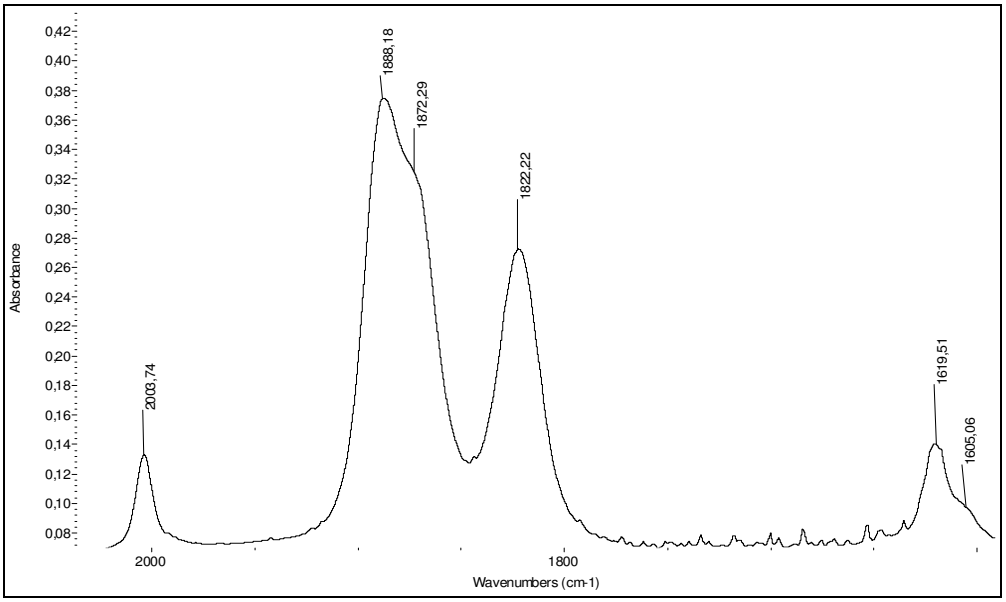

Figure 4.2.7. The IR Spectrum of $Cr(CO)_4$(BFEDA) in CH_2Cl_2 taken at room temperature

In the IR spectrum of the complex, $[Cr(CO)_4(BFEDA)]$, four absorption bands at 2004, 1888, 1872, 1822 cm^{-1} are observed for the carbonyl stretching vibrations. The observation of four absorption bands in the CO stretching region indicates a *cis* arrangement of four CO groups in the pseudo-octahedral coordination sphere of the metal. Thus, the $M(CO)_4$ unit in the complex has a local C_{2v} symmetry with the CO stretching modes of $2A_1 + B_1 + B_2$ (Figure 4.2.8).[40]

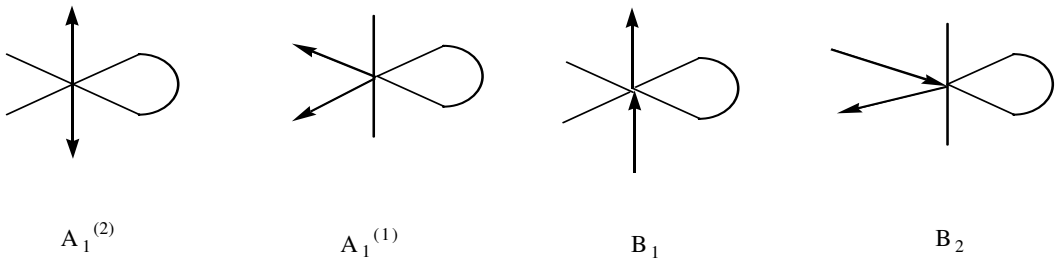

Figure 4.2.8. Symmetry coordinates for the CO stretching vibrational modes in the cis-$M(CO)_4L_2$

The absorption bands at 1620 and 1605 cm^{-1} are assigned to the two possible vibrational modes of the C=N group (Figure 4.2.9). Recall that the ligand shows an absorption band at 1646 cm^{-1} for the same vibration. This indicates a significant weakening of the C=N bond upon coordination. Consequently, the BFEDA ligand becomes more liable to the nucleophilic attack when coordinated than in the free molecule, because of the metal→ imine π bonding.

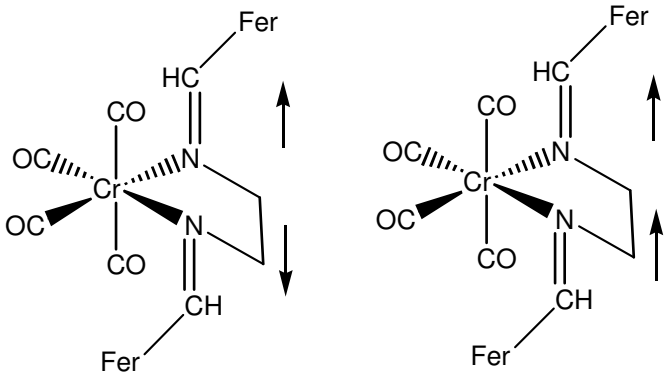

Figure 4.2.9. The C=N stretching modes of $Cr(CO)_4(BFEDA)$

The comparison of the carbonyl region of the IR spectra of $Cr(CO)_4$(BFEDA) (Figure 4.2.7) and $Cr(CO)_4(\eta^{2:2}$-COD) (Figure 4.2.6) shows that the CO stretching frequencies of $Cr(CO)_4$(BFEDA) are lower than the respective bands of $Cr(CO)_4(\eta^{2:2}$-COD) (Table 4.2.1). This indicates that the BFEDA ligand has π-accepting ability less than the olefins.

Table 4.2.1. IR frequencies of $Cr(CO)_4(\eta^{2:2}$-COD) and $Cr(CO)_4$(BFEDA) (λ, cm^{-1}).

Compound	$A_{1(2)}$	B_1	$A_{1(1)}$	B_2
$Cr(CO)_4$ ($\eta^{2:2}$-COD)	2022	1940	1924	1883
$Cr(CO)_4$BFEDA	2011	1894	1875	1824

Table 4.2.2 shows the elemental analysis results belonging to carbon and hydrogen atoms in the molecule and gives a comparison between experimental and theoretical values of these atoms in the $Cr(CO)_4$(BFEDA).

Table 4.2.2. Elemental analysis values and theoretical mass percentages of the carbon and hydrogen atoms in the $Cr(CO)_4$(BFEDA).

Atom	**Experimental**	**Theoretical**
Carbon	54.9	54.5
Hydrogen	3.9	3.8
Nitrogen	4.0	4.5

The ^{1}H-NMR and ^{13}C-{^{1}H}-NMR spectra give all the expected peaks for $Cr(CO)_4$(BFEDA). Although the ^{1}H-NMR spectrum of $Cr(CO)_4$(BFEDA) shows the same pattern as the ^{1}H-NMR spectrum of the free BFEDA molecule. Since the electron-withdrawing carbonyl groups cause a decrease on the electron density of the imine moiety, corresponding peaks are observed at lower fields in the complex than that in the free BFEDA molecule (Figure 4.2.10). Whereas two singlets for the protons of the monosubstituted cyclopentadienyl ring are observed at 4.588 (H3, H4) and 5.091 ppm (H2, H5), one singlet for the five equivalent protons of the unsubstituted cyclopentadienyl ring is observed at 4.258 ppm with an intensity ratio of 2:2:5. The imine hydrogen (–C**H**=N–) gives a signal at 8.503 ppm. Also, the signal at 3.666 ppm belongs to protons of the methylene groups.

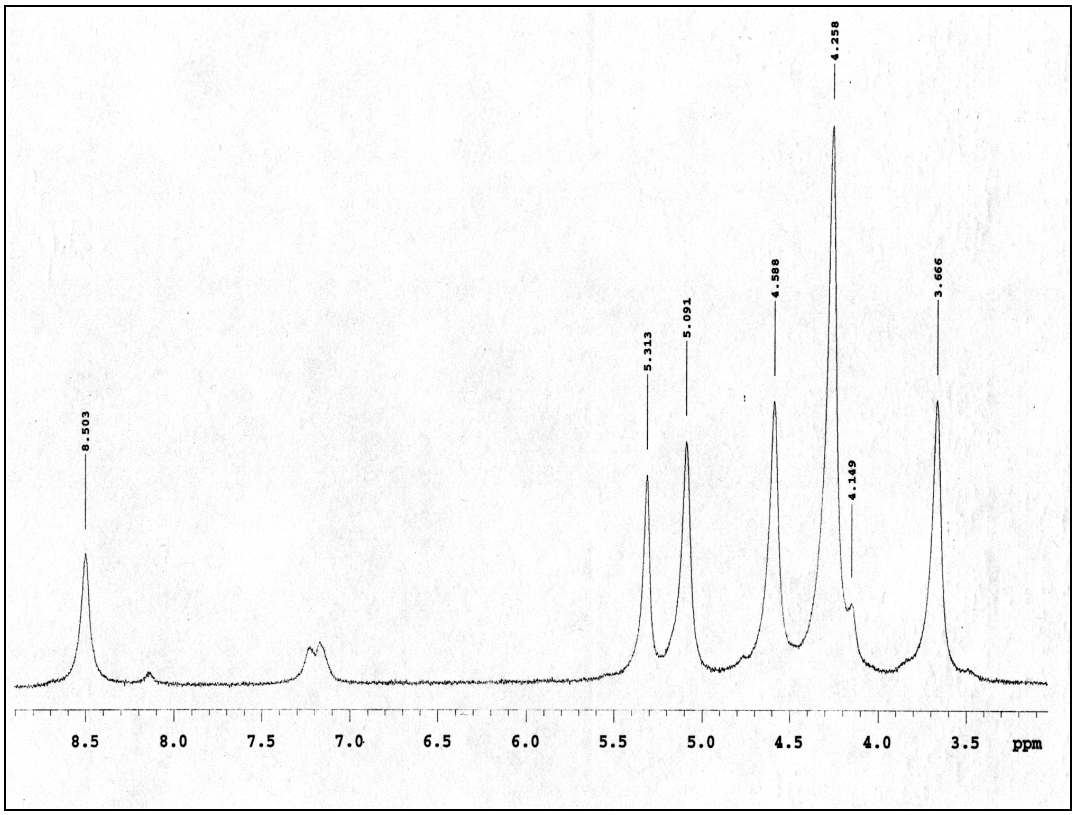

Figure 4.2.10. ^{1}H-NMR Spectrum of $Cr(CO)_4$(BFEDA) in CD_2Cl_2 . Note the signal at 7.2 ppm is due to the toluene solvent.

The ^{13}C-{^{1}H}-NMR spectrum of the $Cr(CO)_4$(BFEDA) (Figure 4.2.11), again gives a signal pattern for the BFEDA ligand similar to the one observed for the free BFEDA molecule. However, the signals of the complex are shifted towards lower field except the one of C1 (δ = 78.296 ppm) which shows a shift of 1.6 ppm toward higher magnetic field. It is worth to note that the signals of the C3 and C4 (δ = 72.304 ppm) are deshielded more than carbons of the unsubstituted ring with respect to the values of the free BFEDA molecule {δ(C3, C4) = 68.833 ppm, $\delta(C_{unsubst})$ = 69.404 ppm} and have their position just near the signals of C2 and C5 (δ = 72.504 ppm). Carbons of the methylene groups of the imine moiety give a signal at 66.130 ppm. The signal corresponding to the imine carbons of the –**C**H=N– groups is observed at 171.070 ppm.

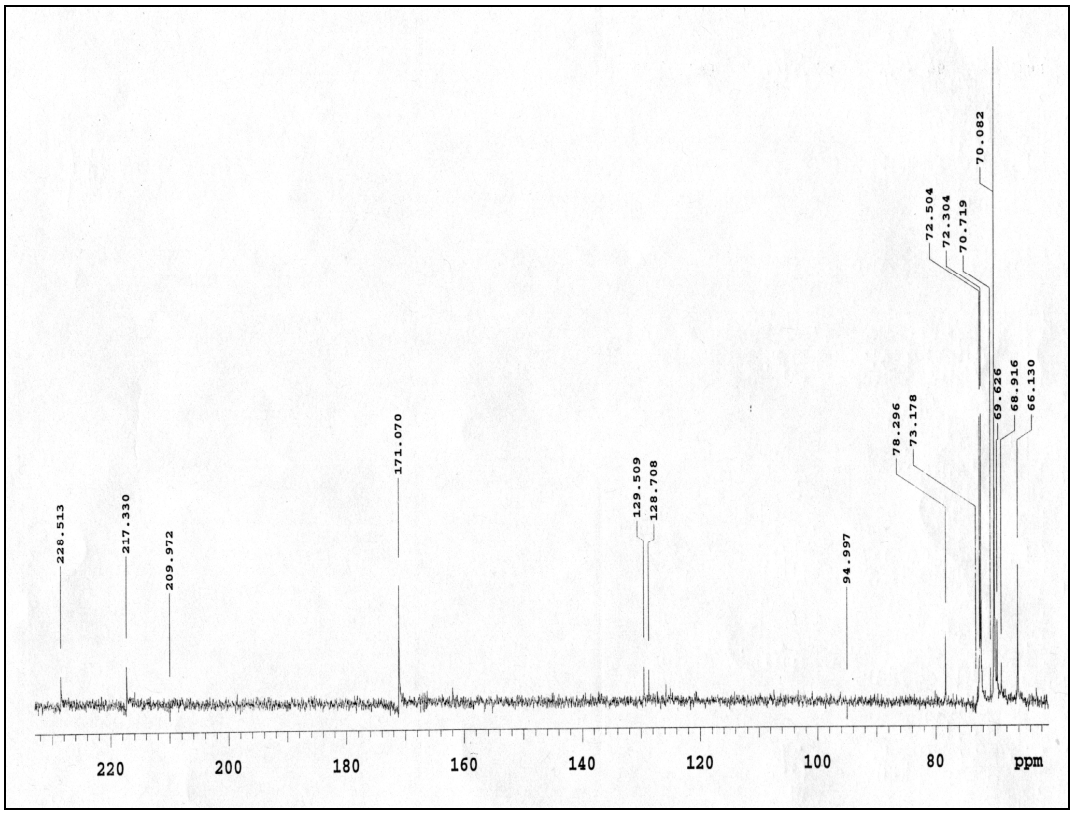

Figure 4.2.11. ^{13}C-NMR Spectrum of $Cr(CO)_4$(BFEDA) in CD_2Cl_2. Note the signals at 68.916, 69.626, 70.082 ppm belong to free BFEDA molecule.

From the deshielding of the carbon atoms in the complex, with the exception of C1, we can conclude that BFEDA is a σ-donor ligand rather than a π-acceptor ligand (in the case of COD in $Cr(CO)_4(\eta^{2:2}$-COD)), and when coordinated, due to conjugation, electron transfer from ligand to Cr is observed. As a result of this interaction, electron density of cyclopentadienyl rings and C=O bond decrease but electron density on the bond between C1 and imine carbon increase and shielding of C1 is observed. Also, in ^{1}H-NMR spectrum of $Cr(CO)_4$(BFEDA), it can also be concluded that, rather than electron-withdrawing carbonyl groups, this σ-donation ability of the ligand is the main reason for the deshielding of the protons in the complex.

Furthermore, the ^{13}C-{^{1}H}-NMR gives two signals at 228.513 and 217.330 ppm for the carbonyl groups with a relative intensity ratio of 1:1. This is in accord with the cis arrangement of the four carbonyl ligands concluded from the IR spectrum of the $Cr(CO)_4$(BFEDA). The ^{13}C carbonyl resonance at lower field (δ = 228.513 ppm) is attributed to the CO groups in the equatorial positions, leaving the one at higher field (δ = 217.330 ppm) for the axial CO groups. This is in accord with the previously reported ordering of signals associated with the axial and equatorial CO groups in $M(CO)_4$(α-diimine) complexes, δ(CO-eq) > δ(CO-ax).[41]

In table 4.2.3, ^{13}C-NMR chemical shifts (δ, ppm) of BFEDA and $Cr(CO)_4$(BFEDA) as well as the coordination shift {(Δδ = δ (coordinated ligand) – δ (free ligand)}[42] values are shown. The coordination shift to lower magnetic field may be explained by the fact that the BFEDA molecule is a good σ-donor but a weak π-acceptor ligand. Therefore it transfers electron to the empty orbitals of the metal through σ-bonding when it is coordinated to chromium fragment. As expected from the closeness of the carbon atoms to the coordination site, the highest coordination shift value belongs to the carbon atom of the imine. The higher coordination shift values of the C3 and C4 than carbons of the

unsubstituted ring can be assigned to the strong interaction with the Cr metal through conjugation. Also, when coordinated, C2, C3, C4 and C5 have very similar chemical shifts. This might be attributed to the delocalization of the electrons on the substituted cyclopentadienyl ring as the electron density decreases.

Table 4.2.3. ^{13}C-{^{1}H}-NMR chemical shifts (δ, ppm) of BFEDA and $Cr(CO)_4$(BFEDA), and coordination shift values (Δδ, ppm).

	δ(C1)	δ(C2,5)	δ (C3,4)	δ($C_{unsubst}$)	δ(**C**H_2)	δ(**C**=N)
BFEDA	80.006	70.711	68.833	69.404	61.538	162.673
$Cr(CO)_4$(BFEDA)	78.296	72.504	72.304	70.082	66.130	171.070
Coordination shift, Δδ (ppm)	-1.710	1.793	3.471	0.678	4.592	8.397

In the UV-VIS spectrum of $Cr(CO)_4$BFEDA (Figure 4.2.12) the bands at 233 and 269 nm are assigned to the charge transfer transitions of the ferrocenyl moiety. The bands observed at 340 and 450 nm are attributed to d-d transitions.[43]

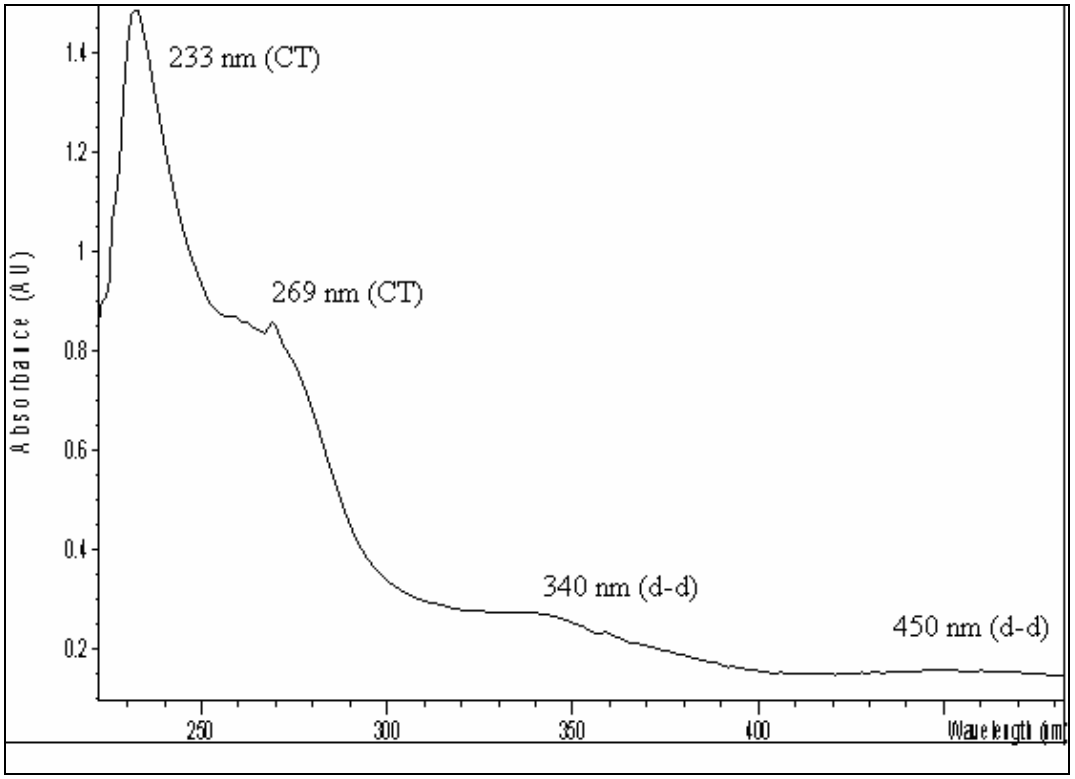

Figure 4.2.12. The UV-VIS Spectrum of $Cr(CO)_4$(BFEDA) in CH_2Cl_2

The mass spectrum (Figure 4.2.13) shows the molecular peak of the complex at m/z = 616 with the characteristic isotope distribution. This value of m/z = 616 is exactly in agreement with the theoretical molecular weight, which is also 616.

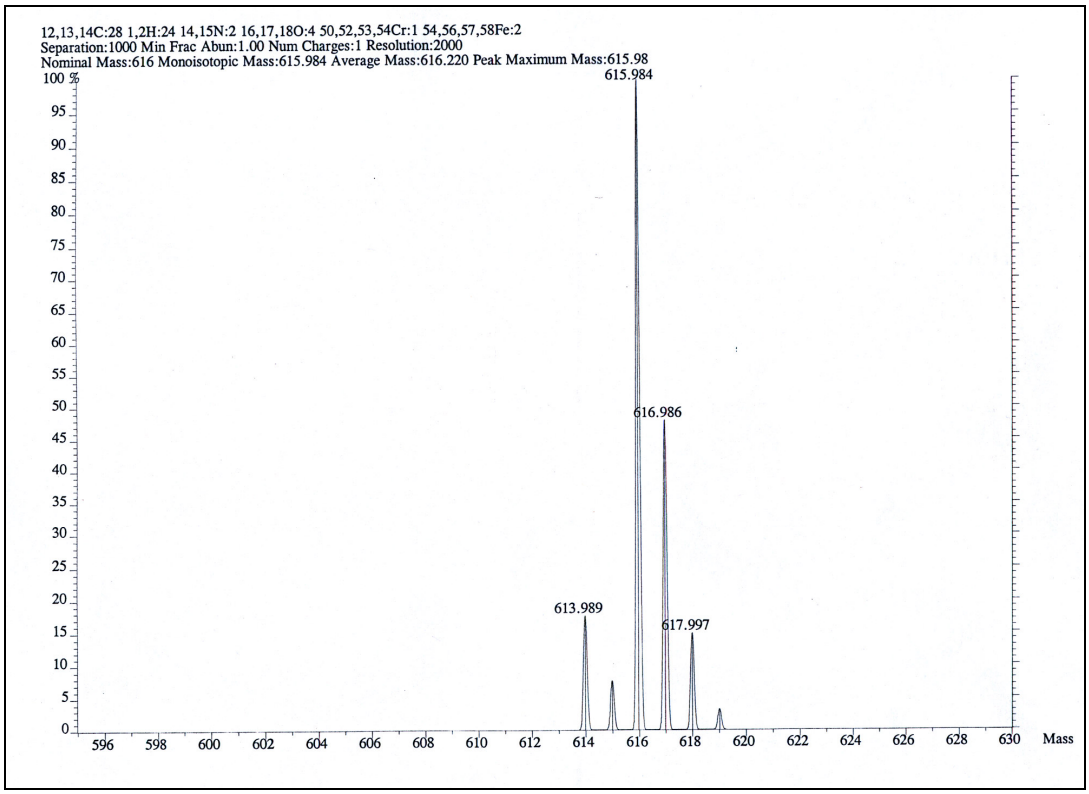

Figure 4.2.13. The Mass Spectrum of $Cr(CO)_4$(BFEDA)

Figure 4.2.14 illustrates the cyclic voltammogram of $Cr(CO)_4$(BFEDA) in CH_2Cl_2. It exhibits three oxidations at 0.263, 0.610 and 0.765 V. Note that, Ag-wire was used as the reference electrode. The oxidation peak at 0.263 V is assigned to the redox processes involving the Cr fragment, whereas the oxidation peaks at 0.610 and 0.765 V are assigned to ferrocenyl oxidations. The separation of the two sequential oxidations of ferrocenyl groups is 0.155 V. These two oxidations are not resolved from each other in the free BFEDA molecule. The separation of them upon complexation means that there is a communication between two centers. It has to be noted that the presence of the $Cr(CO)_4$ fragment exerts a significant electron-withdrawing effect on the BFEDA ligand making the oxidation of the two ferrocenyl groups to shift towards more positive potential values by about 0.10 - 0.15 V.[44] Recall that ferrocenyl oxidation of the free BFEDA molecule occurs at 0.567 V.

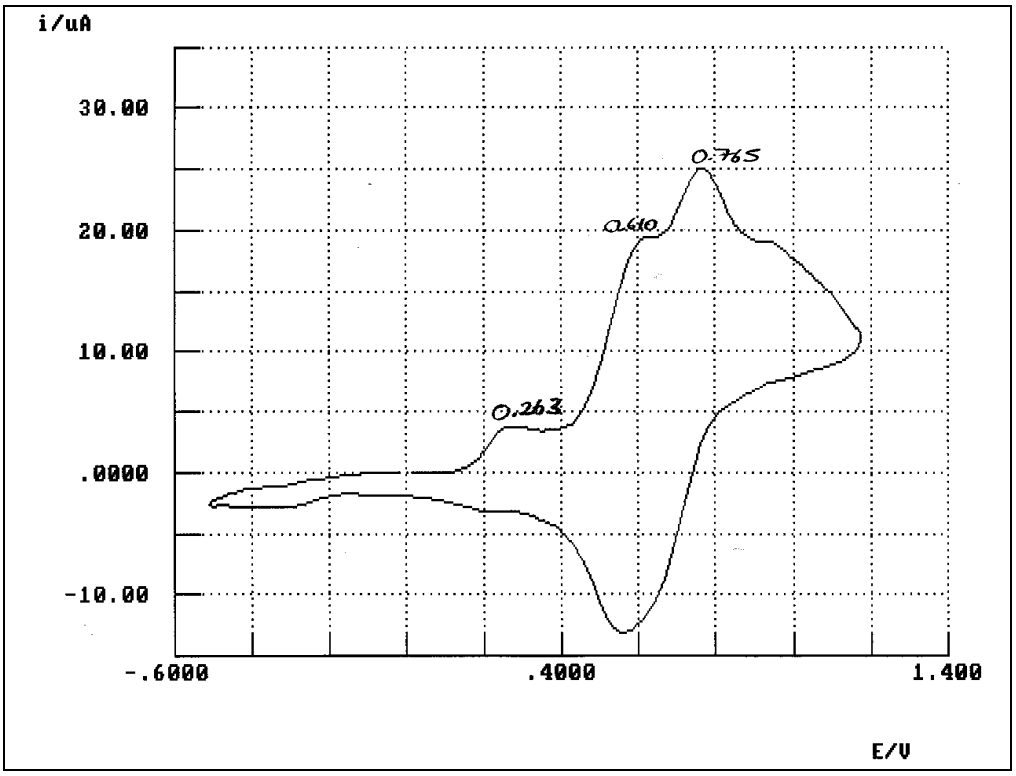

Figure 4.2.14. CV of [$Cr(CO)_4$(BFEDA] taken at room temperature in CH_2Cl_2 solution containing the electrolyte, tetrabutylammonium tetrafluoroborate.

The electrochemical oxidation of the complex, $Cr(CO)_4$(BFEDA) was carried out at the peak potential in CH_2Cl_2 at 0 °C in order to prevent volatilization of the solvent. The spectral changes were followed in-situ by UV-VIS spectrophotometer. As there were three oxidation steps which was determined by cyclic voltammetry measurements, the electrolytic oxidation of the complex was divided into three parts:

1. Oxidation of the chromium fragment, changing the oxidation state of chromium from (0) to (+1):

$$Cr(CO)_4(BFEDA) \rightarrow Cr^{+}(CO)_4(BFEDA) + e^{-}$$

2. First oxidation of the ferrocenyl moiety:

$$Cr^{+}(CO)_4(BFEDA) \rightarrow Cr^{+}(CO)_4(BFEDA^{+}) + e^{-}$$

3. Second oxidation of the ferrocenyl moiety, changing the oxidation state of iron centers from (+2) to (+3):

$$Cr^{+}(CO)_4(BFEDA^{+}) \rightarrow Cr^{+}(CO)_4(BFEDA^{2+}) + e^{-}$$

As soon as the electrochemical oxidation of the $Cr(CO)_4$(BFEDA) came to end, electrochemical reduction of the $Cr(CO)_4$(BFEDA) was performed to see whether the original molecule would be regenerated or not:

$$Cr^{+}(CO)_4(BFEDA^{2+}) + 3e^{-} \rightarrow Cr(CO)_4(BFEDA)$$

In the first part (Figure 4.2.15) which mainly corresponds to redox processes of the chromium fragment, no important changes were observed as the bands in the spectrum belong to ferrocenyl moiety.

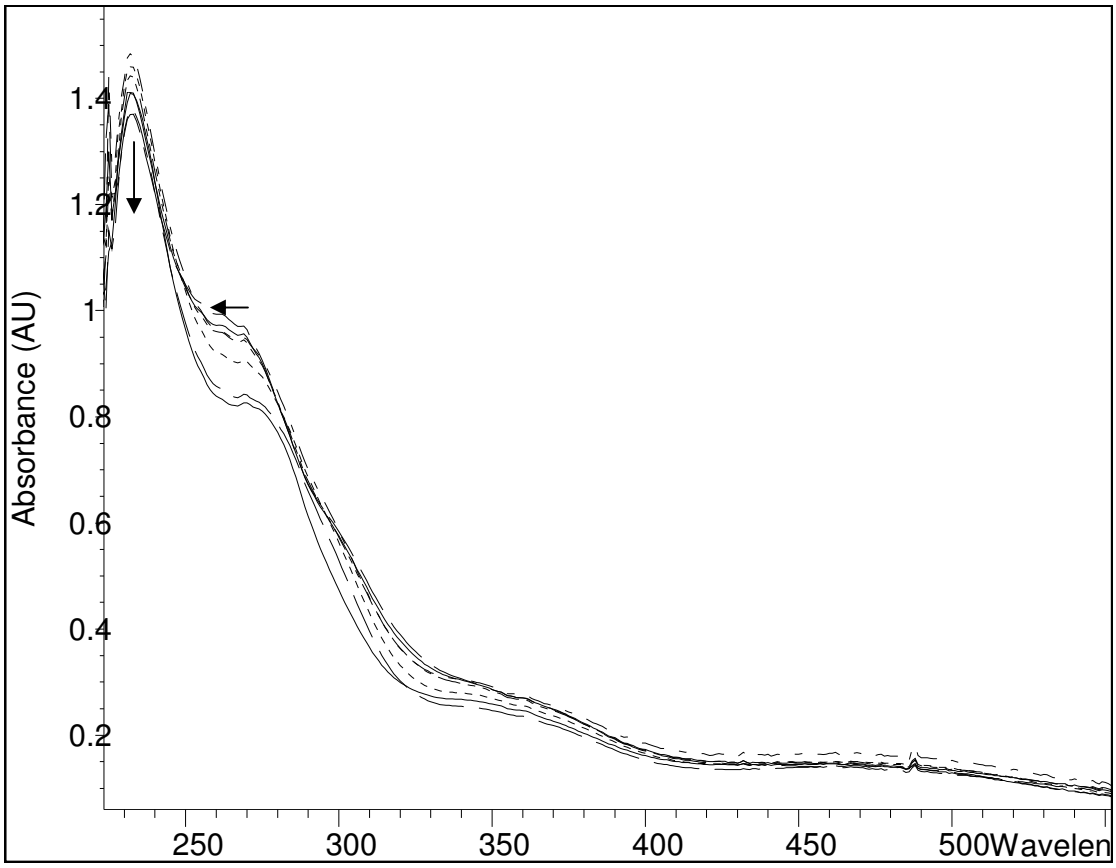

Figure 4.2.15. The UV-VIS electronic absorption spectra for the first oxidation of $Cr(CO)_4$(BFEDA) at 0 °C, recorded during electrolytic oxidation of the complex at 0.700 V in CH_2Cl_2 solution containing the electrolyte, tetrabutylammonium tetrafluoroborate

In the second part (Figure 4.2.16) which corresponds to first oxidation of ferrocenyl moiety, a new band at 256 nm formed, the band at 301 nm shifted towards right with increasing in intensity, the intensity of the band at 362 nm increased and the intensity of the band at 232 nm decreased.

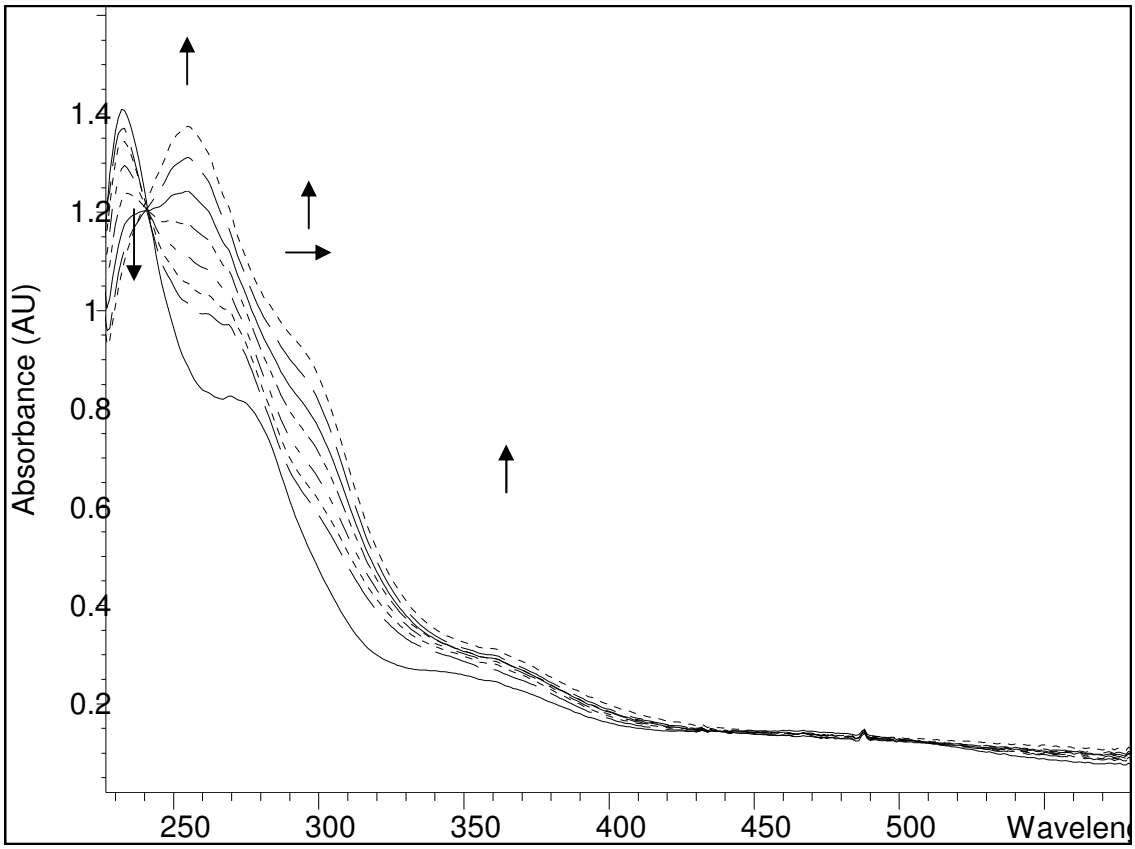

Figure 4.2.16. The UV-VIS electronic absorption spectra for the second oxidation of $Cr(CO)_4$(BFEDA) at 0 °C, recorded during electrolytic oxidation of the complex at 0.700 V in CH_2Cl_2 solution containing the electrolyte, tetrabutylammonium tetrafluoroborate

In the final part (Figure 4.2.17) which corresponds to the second oxidation of the ferrocenyl moiety, the intensities of the bands at 301 nm and 362 nm continued to increase and the band at 450 nm made a shift towards higher frequencies.

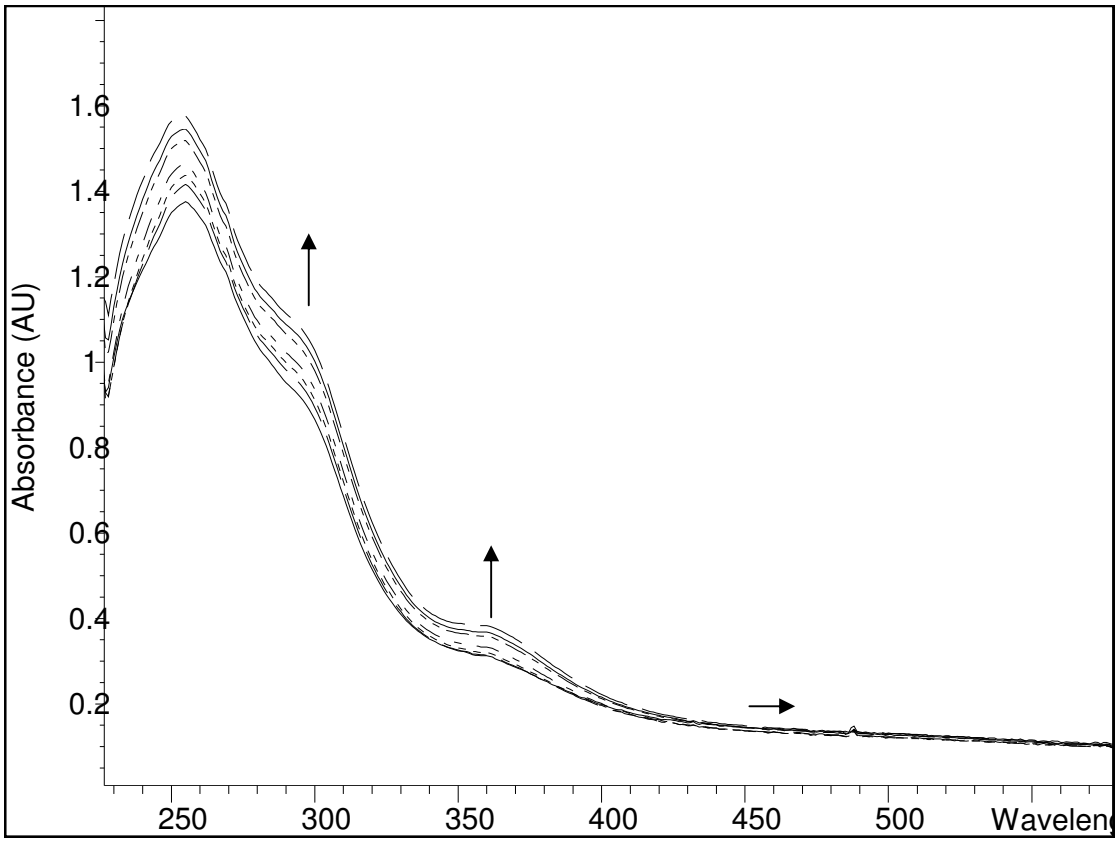

Figure 4.2.17. The UV-VIS electronic absorption spectra for the third oxidation of $Cr(CO)_4$(BFEDA) at 0 °C, recorded during electrolytic oxidation of the complex at 1.100 V in CH_2Cl_2 solution containing the electrolyte, tetrabutylammonium tetrafluoroborate

The overall change in the electronic absorption spectra during the oxidation is shown in Figure 4.2.18. It is observed that the changes in the spectrum began mainly during second part of the oxidation, and generally the second and the third oxidation have similar trends. This might be due to the fact that the ferrocenyl oxidations are very close in value (0,610 and 0,765 V) and these oxidations might occur at the same time.

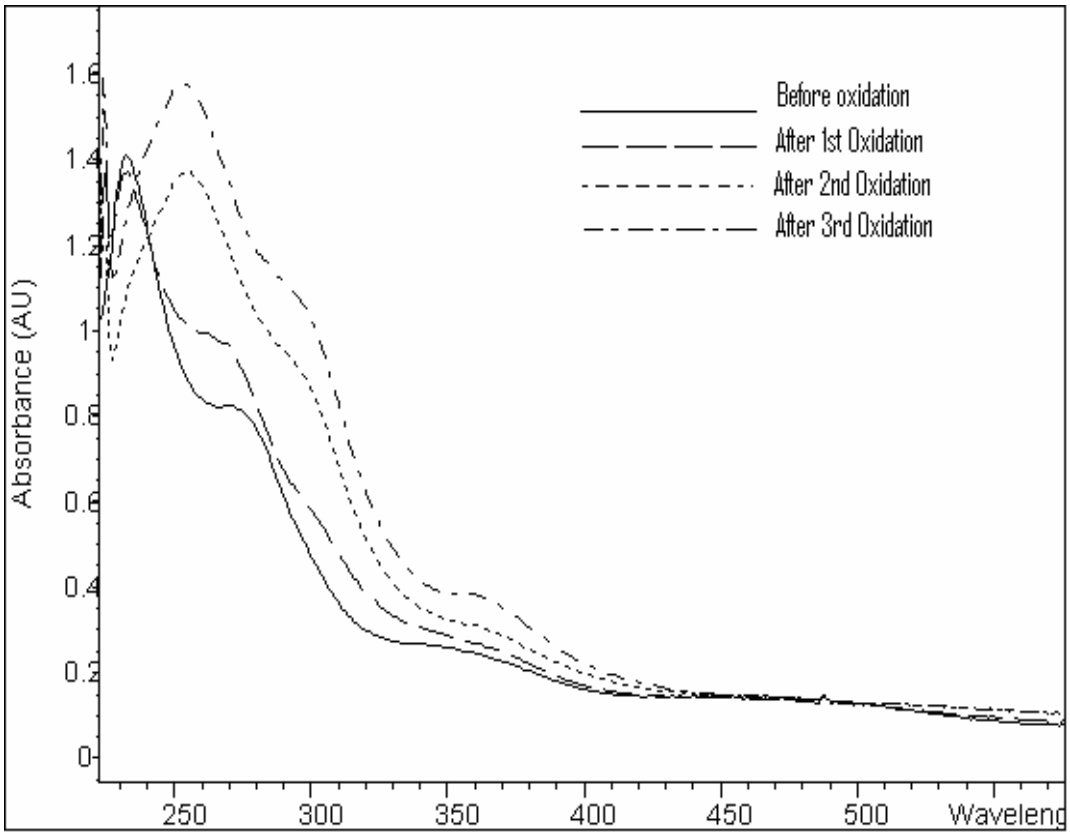

Figure 4.2.18. The UV-VIS electronic absorption spectra of $Cr(CO)_4$(BFEDA) at 0 °C, recorded during electrolytic oxidation of the complex in CH_2Cl_2 solution containing the electrolyte, tetrabutylammonium tetrafluoroborate

The spectral changes observed in UV-VIS spectrum during the oxidation of $Cr(CO)_4$(BFEDA) are not informative to identify the product. However, the observed changes are assigned to electrons taken from Fe centers, indicating ferrocene moiety turns to ferricenium moiety (Scheme 4.2.1).[45] It is important to note that removal of the electrons from the Fe centers in the free BFEDA molecule occurs at the same potential. The two equivalent iron centers are far away from each other to communicate electronically and there exists no conjugation between them. But, in the complex, there exists an interaction between Fe centers through the chromium center due to conjugation, which is also evidenced in cyclic voltammetry by observing two oxidation peaks instead of one oxidation peak.

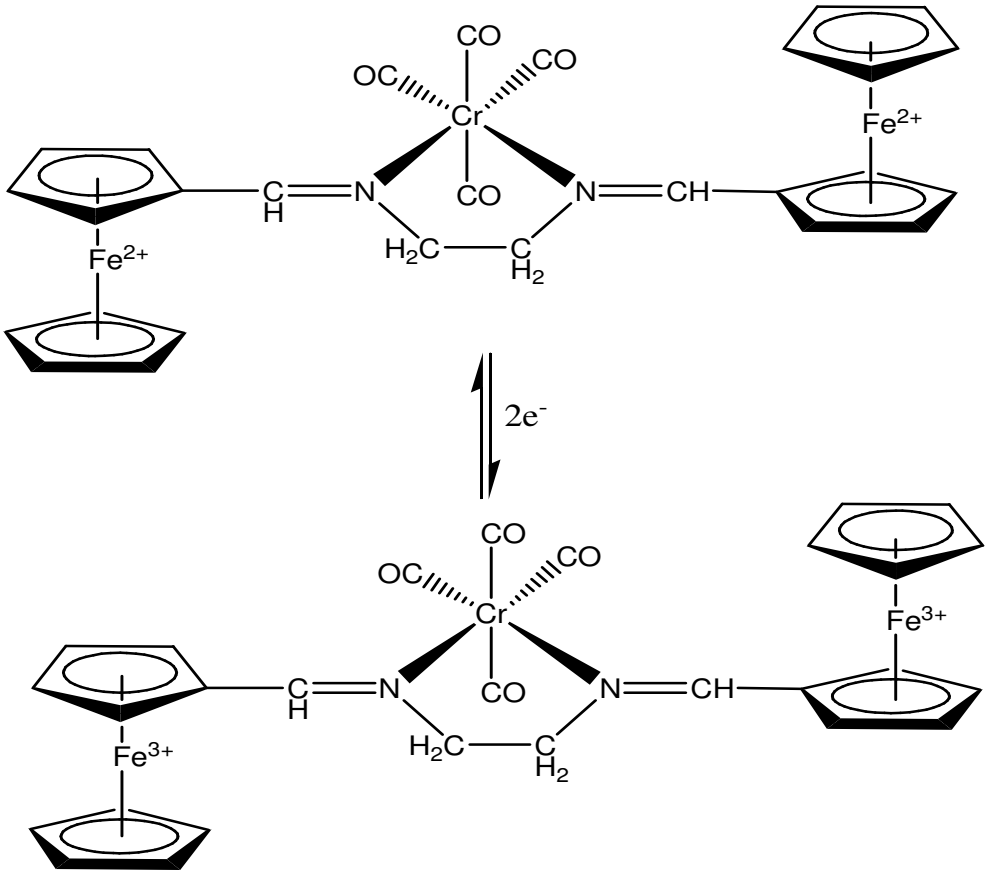

Scheme 4.2.1. Electron transfers from Fe centers during oxidation of the complex

After the oxidation process was over, the electrochemical reduction of the complex was carried out in the same electrolyte solution. After two electron transfer have been completed, it was observed that the original complex was regenerated (Figure 4.2.19).

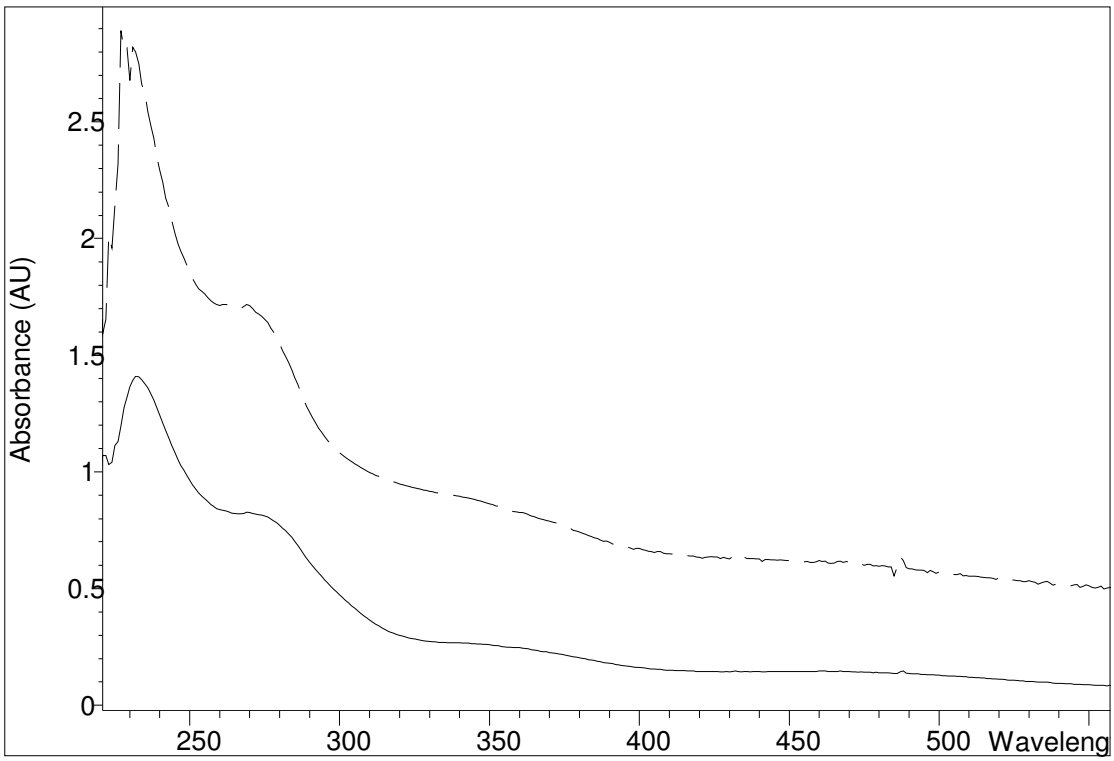

Figure 4.2.19. The UV-VIS electronic absorption spectra of $Cr(CO)_4$(BFEDA) recorded before the electrolysis and at the end of the electrochemical reduction (the dashed line)

Finally, the electrochemical oxidation of the complex, $Cr(CO)_4$(BFEDA) was carried out at a constant current and the changes were followed by means of IR spectroscopy (Figure 4.2.20). During oxidation, as the bands belonging to $Cr(CO)_4$(BFEDA) complex were decreasing in intensity, new bands at 1980 and 1923 cm^{-1} were forming. The band at 1980 cm^{-1} was easily assigned to carbonyl stretching of a hexacarbonyl complex indicating the formation of $Cr(CO)_6$. During oxidation as the electron density on the complex decreases, electron density on the chromium atom decreases, too. This will cause a weakening of Cr → CO π-backbonding. These bonding changes should have an influence on the ν(CO) vibration by shifting them to higher frequencies.[46] The band at 1923 cm^{-1} assigned to these CO groups. Also a new band at 1713 cm^{-1} was observed. This band can be assigned to a carbonyl cluster or a bridging carbonyl molecule. Although reported M – CO – M structures have this band between 1750 and 1900 cm^{-1}, it must be added that the vibrations of bridging carbonyls have not been investigated as those of terminal groups.[40] Also formation of the bands at 1642 and 1680 cm^{-1} are assigned to free ligand and aldehyde formation, respectively.

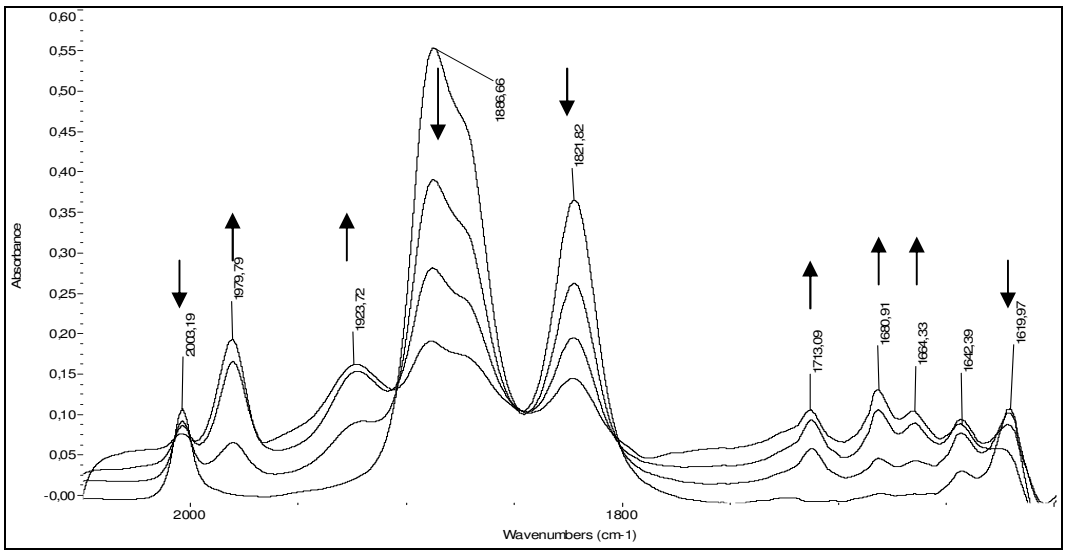

Figure 4.2.20. The IR spectra of $Cr(CO)_4$(BFEDA) at room temperature, recorded during electrolytic oxidation of the complex in CH_2Cl_2 solution containing the electrolyte, tetrabutylammonium tetrafluoroborate

CHAPTER 5

CONCLUSIONS

The N,N'-bis(ferrocenylmethylene)ethylenediamine (BFEDA) was prepared from the reaction of ferrocenecarboxaldehyde and ethylenediamine in benzene solution by using a Dean-Stark apparatus and characterized by IR, Raman and NMR spectroscopies. This diimine molecule containing two ferrocenyl moieties was employed as a bidentate ligand in the synthesis of tetracarbonyl [N,N'-bis(ferrocenylmethylene)ethylenediamine]chromium(0), $Cr(CO)_4$(BFEDA).

In order to synthesize $Cr(CO)_4$(BFEDA), first photolysis of hexacarbonylchromium(0), $Cr(CO)_6$, in the presence of BFEDA was tried. However, the monosubstitution product $Cr(CO)_5$(BFEDA) forms prior to the $Cr(CO)_4$(BFEDA) complex, the separation of which could not be achieved.

In the second attempt, the thermal substitution of a metastable complex, $Cr(CO)_5$(THF), was used to form the $Cr(CO)_4$(BFEDA) from its reaction with BFEDA. However this reaction yields also a mixture of mono- and disubstitution products.

Finally, $Cr(CO)_4$(BFEDA) was synthesized and isolated for the first time from the ligand exchange reaction of tetracarbonyl($\eta^{2:2}$-1,5-cyclooctadiene)chromium(0), $Cr(CO)_4(\eta^{2:2}$-COD) with BFEDA in toluene solution.

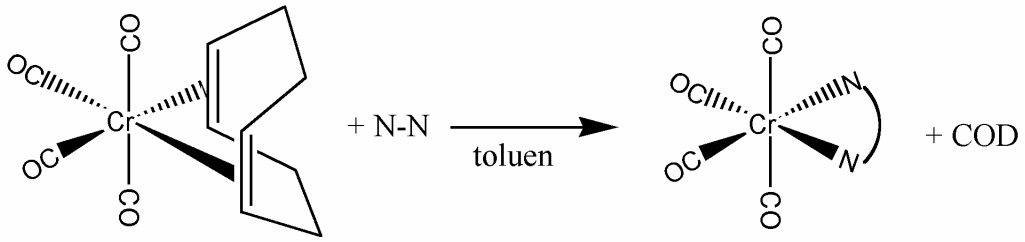

$Cr(CO)_4$(BFEDA), like many other organometallic molecules, is found to be air sensitive and tends to decompose when exposed to air or moisture. Furthermore, the π-backbonding from metal to π^*-orbital of the imine weakens the C=N bond, and as a result, this bond becomes very susceptible to be attacked by water to hydrolyze to ferrocenecarboxaldehyde and ethylenediamine.

$Cr(CO)_4$(BFEDA) was fully characterized by elemental analysis, UV-VIS, IR, ^{1}H-NMR, ^{13}C-{^{1}H}-NMR and Mass spectroscopies. The IR spectrum of $Cr(CO)_4$BFEDA displays four CO stretching bands due to C_{2v} local symmetry and one C=N stretching band. The C_{2v} symmetry of $Cr(CO)_4$ fragment was also confirmed by ^{1}H-NMR and , ^{13}C-{^{1}H}-NMR spectroscopies.

IR and ^{13}C-{^{1}H}-NMR studies show that, BFEDA molecule is a σ-donor ligand rather than a π-acceptor ligand. This σ-donation ability of BFEDA upon coordination causes a decrease in the electron density of all the atoms in the BFEDA fragment except C1. Another consequence of the σ-donation from BFEDA to $Cr(CO)_4$ fragment is the weakening of the triple bond of the carbonyl groups.

The electrochemical behavior of $Cr(CO)_4$(BFEDA) was also studied by using cyclic voltammetry and the mechanism of electrode reaction was investigated by in-situ UV-VIS and IR spectroscopic measurements. These studies reveal that the three redox active centers (chromium and iron centers) of $Cr(CO)_4$(BFEDA) are communicating with each other electronically. However, spectroelectrochemical studies did not give the full characterization of the electrochemical oxidation products, and instability of the electrolytic products disabled further studies.

.

REFERENCES

1. Bochmann, M., *Organometallics 1: Complexes with transition metal-carbon σ-bonds*, Oxford Science Publications.

2. Zeise, W. C., *Pogg Annalen*, **1827**, 9, 632.

3. Kealy, T. J.; Pauson P. J., *Nature*, London, **1951,** 168, 1039.

4. Miller, S. A.; Tebboth J. A.; Tremaine J. F., *Journal of Chem. Soc.*, **1952**, 632.

5. Wilkinson, G.; Rosenblum, M.; Whitting M. C.; Woodword, R. B., *J. Am. Chem. Soc.,* **1952**, 74, 21.

6. Coates, G. E.; Green, M. L. H.; Powwell, P.; Wade K., *Principles of Organometallic Chemistry*, Methwen Co. Ltd., London, **1968**, 1.

7. Lin, K.; Song, M.; Zhu, Y.; Wu, Y., *Journal of Organometallic Chemistry*, **2001**, 637, 27.

8. Eisch, J., The Chemistry of Organometallic Compounds: The Main Group Elements, Academic Press, New York, **1967**.

9. Togni, A.; Hayashi, T., *Ferrocenes — Homogeneous Catalysis*, *Organic Synthesis, Materials Science*, VCH, Weinheim, **1995**.

10. Bear, P. D.; Smith, D. K., *Prog. Inorg. Chem.*, **1997**, 46, 1.

11. Miller, J. S.; Epstein, A. J., *Angew. Chem. Int. Ed. Engl.*, **1994**, 34, 385.

12. Long, N. J., *Angew. Chem. Int. Ed. Engl.*, **1995**, 35, 21.

13. Coles, H. J.; Meyer, S.; Lehmann, P.; Deshenaux, R.; Juaslin, J., *Mater. Chem.*, **1999**, 9, 1085.

14. Özkar, S.; Kayran, C.; Demir, N., *Journal of Organometallic Chemistry*, **2003**, 688, 62.

15. Cullen, W. R.; Woollins, J. D., *Coord. Chem. Rev.*, **1981**, 39, 1.

16. Lopez, C.; Caubet, A.; Solans, X.; Font-Bardia, M., *Journal of Organometallic Chemistry*, **2000**, 598, 87.

17. Riera, X.; Amparo, C.; Lopez, C.; Moreno, V., *Polyhedron*, **1999**, 18, 2549.

18. Lopez, C. W. R.; Caubet, A.; Solans, X.; Font-Bardia, M.; Bosque, R., *Journal of Organometallic Chemistry*, **1999**, 577, 292.

19. Constable, E. C.; *Metals and Ligand Reactivity*, Ellis Howard Ltd, Chichester, **1990**.

20. Süss-Fink G.; Meister G., *Adv. Organomet. Chem.*, **1993**, 35, 41.

21. Cotton F. A.; Wilkinson G., *Advanced Inorganic Chemistry 5th Edition,* John Wiley & Sons, New York, **1988**.

22. Pickett, C. J.; Pletcher, D., *J. C. S. Chem. Comm*., **1974,** 6608.

23. Plambeck, J. A., *Electroanalytical Chemistry: Basic Principles and Applications*, John Wiley & Sons, New York, **1982**, 229.

24. Connely, N. G.; Geiger, W. E., *Advances in Organometalic Chemistry*; Academic Press, New York, **1984,** 23, 1**.**

25. Hamann, C. H.; Hamnett, A.; Vielstich, W., *Electrochemistry*, Wiley-VCH, Weinheim, **1998**.

26. Benito, A.; Cano, J.; Manez, R. M.; Soto, J.; Paya, J.; Lloret, F.; Julve, M.; Faus, J.; Marcos, M. D.; *Inorg. Chem.*; **1993**, 32, 1197.

27. Zhang, H.; Lei, J.; Chen, Yi.; Lin, L.; Wu, Q.; Zhang, H., *Synth. React. Inorg. Met. Org. Chem.*, **2001**, 31(6), 1053.

28. Shriver, D. F.; Atkins, P. W; Langford, C. H., *Inorganic Chemistry*, Butler and Taner Ltd., **1991**.

29. Solomons, G.; Fryhle, C., *Organic Chemistry – Seventh Edition*, John Wiley& Sons, Inc., **2000**.

30. Komiya, S., *Synthesis of Organometallic Compounds*, John Wiley & Sons, Chichester, **1997**.

31. Lopez, C.; Sales, J.; Solans, X.; Zquiak, R., *J. Chem. Soc.*, Dalton Trans., **1992**, 2321.

32. Bosque, R.; Lopez, C.; Sales, J.; Solans, X.; Font-Bardia, M., *J. Chem. Soc.*, Dalton Trans., **1994**, 735.

33. Kotzian, M.; Kreiter, C. G.; Özkar, S., *J. Organomet. Chem.*, **1982**, 229.

34. Tekkaya, A.; Kayran, C.; Özkar, S.; Kreiter, C. G., *Inorg. Chem.,* **1994**, 33, 2439.

35. Ebsworth, E. A. V.; Rankin, D. W. H.; Cradock, S.; *Structural Methods in Inorganic Chemistry*, **1994**.

36. Pickett T. E.; Richards C. J., *Tetrahedron Letters*; **1999**, 40**,** 5251**.**

37. Rohmer, M. M.; Veillard, A.; Wood, M. H., *Chemical Physics Letters*, **1974**, 29, 466.

38. Strohmeier, W.; Schonauer, G., *Chem. Ber.*, **1961**, 94, 1346.

39. Kayran, C.; Kozanoğlu, F.; Özkar, S.; Saldamlı, S.; Tekkaya, A.; Kreiter, C. G.; *Inorganica Chimica Acta*, **1999**, 284, 229.

40. Braterman, P. S., *Metal Carbonyl Spectra,* Academic Press, London , **1975**

41. Grevels, F. W.; Kerpen, K.; Klotzbücher, W. E.; Schaffner, K.; Goddard, R.; Weimann, B.; Özkar, S.; Kayran, C., *Organometallics,* **2001**, 20, 4775.

42. Grim, S. O.; Heatland, D. A.; MacFarlane., *J. Am. Chem. Soc*., **1967**, 89, 5573.

43. Sohn, Y. S.; Hendrickson D. N.; Gray, H. B., *J. Am. Chem. Soc.*, **1971**, 93, 3603.

44. Bildstein, B.; Malaun, M.; Kopacka, H.; Fontani, M.; Zanello P., *Inorganic Chimica Acta*, **2000,** 16, 300**.**

45. Farrell I. R., *Inorg. Chim. Acta*, **2001**, 318, 143.

46. Vlcek, A., *Coordination Chemistry Reviews*, **2002**, 230, 225.

APPENDIX 1

UV-VIS Spectra of free BFEDA molecule was taken in 2.0 x 10^{-5} M CH_2Cl_2 solution at room temperature.

At 230 nm, $A = \varepsilon_{230\ nm}.b.c$

$0.593 = \varepsilon_{230\ nm}$ x 0.00002 mole/L

$\varepsilon_{230\ nm} = 2.965 \times 10^4$ L/mole.cm

At 274 nm, $A = \varepsilon_{274\ nm}.b.c$

$0.330 = \varepsilon_{274\ nm}$ x 0.00002 mole/L

$\varepsilon_{274\ nm} = 1.650 \times 10^4$ L/mole.cm

At 330 nm, $A = \varepsilon_{330\ nm}.b.c$

$0.055 = \varepsilon_{330\ nm}$ x 0.00004 mole/L

$\varepsilon_{330\ nm} = 0.275 \times 10^4$ L/mole.cm

At 460 nm, $A = \varepsilon_{460\ nm}.b.c$

$0.021 = \varepsilon_{460\ nm}$ x 0.00004 mole/L

$\varepsilon_{460\ nm} = 0.105 \times 10^4$ L/mole.cm

UV-VIS Spectra of $Cr(CO)_4$BFEDA molecule was taken in 5.0 x 10^{-4} M CH_2Cl_2 solution at room temperature.

At 233 nm, $A = \varepsilon_{233\ nm}.b.c$

$1.566 = \varepsilon_{233\ nm}$ x 0.00004 mole/L

$\varepsilon_{233\ nm} = 3.915 \times 10^4$ L/mole.cm

At 269 nm, $A = \varepsilon_{269\ nm}.b.c$

$0{,}925 = \varepsilon_{269\ nm}.0{,}00004$ mole/L

$\varepsilon_{269\ nm} = 2.312 \times 10^4$ L/mole.cm

At 340 nm, $A = \varepsilon_{340\ nm}.b.c$

$0.249 = \varepsilon_{340\ nm}$ x 0.00004 mole/L

$\varepsilon_{340\ nm} = 0.623 \times 10^4$ L/mole.cm

At 450 nm, $A = \varepsilon_{450\ nm}.b.c$

$0.106 = \varepsilon_{450\ nm}$ x 0.00004 mole/L

$\varepsilon_{450\ nm} = 0.265 \times 10^4$ L/mole.cm